THUNDER

D1.3: THUNDER

Conceptual design

Demonstrator conceptual design, best practices of seasonal storage and heat source characteristics -

Task 1.1.2 output

Funded by
the European Union

D1.3: THUNDER Conceptual design		
Deliverable number	1.3	
Responsible partner	UNIFI	
Due date of deliverable	30 June 2025	
Actual submission date	30 June 2025	
Version/document history	5.5.2025 Original draft 6.6.2025 (internally) reviewed version	
Authors	UniFI: Andrea Rocchetti, Andrea Zini, Antonio Verzino, Luca Socci, Lorenzo Talluri, Federica Savelli, Martina Lippi.	
Reviewers	VEOLIA	
Work package number and title	WP1: Waste Heat Recovery from Data Centres: framework	
Work package leader	IVL	
Work package participants	UNIFI, IVL, ABILIX, HIREF, SETECHO, UBE, 3SI, VEO, RINA-C, STEELTECH, UNIGE, PCM	
Dissemination level (please select one)		
SEN	Sensitive, limited under the conditions of the Grant Agreement	☐
PU	Public, fully open	☒

Project's information	
Grant Agreement No.	101136186
Project Full Title	THermochemical storage Utilization eNabling Data centre seasonal Energy Recovery
Project Acronym	THUNDER
Start Date	1st of January 2024
End Date	1st of January 2028
Project Coordinator	Matteo Porta (RINA-C)
Project Website	www.thunder.eu

Executive summary

This deliverable represents the final synthesis of Task 1.1.2 of the THUNDER project, which focused on analysing methods for recovering waste heat from a data centre and reusing it in an urban district heating network. The task involved reviewing best practices and identifying the most suitable and effective configuration of the energy chain and the interconnection of its components, to define a reference framework for the project's demonstrator.

The THUNDER project aims to develop a strategy for utilizing thermal energy storage systems to improve the energy efficiency, economic feasibility, and environmental sustainability of recovering waste heat from data centres and reusing it in urban district heating networks. The project identified a key technological solution: the integration of a seasonal thermal storage system, operating through storage and release processes based on thermochemical materials, with an innovative high-temperature heat pump. An approach, "Heat on Wheels", was introduced and implemented, utilizing mobile storage systems to facilitate the connection between energy sources and geographically distant consumers. Then, heat recovery sources, storage systems, and energy reuse solutions are not necessarily physically interconnected via a direct hydraulic link but can connect via mobile storage that the THUNDER project aims to develop, design, and test in its Demonstrator Site in Varna.

The solution developed for the THUNDER project combines seasonal thermal storage and thermal upgrade technologies with a mobile storage and transport system using Phase Change Materials (PCMs).

Task 1.1.2 also involved the development of a numerical simulation tool for modelling the complete energy chain. It models and characterizes each component of the THUNDER energy system and its interconnections. The tool was used to simulate the demonstrator configuration as well as alternative scenarios to assess the replicability of the system in different contexts.

Specifically, the scenarios retained constant parameters for the waste heat source (steady power and temperature) and the thermal user (a district heating network similar to the demonstrator's one).

Four scenarios will be evaluated, representing the extent of the admissible range in terms of "distance" covered by heat on wheel mode and of energy flow management. Scenarios related to a "short distance" and "long distance will be presented, considering two energy control strategies: a case where 5% of the waste heat from the data centre is recovered, and the case where the waste heat generated between June and September is entirely recovered.

Deliverable 1.3 shows that a seasonal thermal storage system based on innovative low temperature thermochemical materials, when integrated with a high-performance thermal upgrade system, can significantly improve the energy, economic, and environmental sustainability of waste heat recovery and reuse in urban areas. Moreover, it concludes that the "Heat on Wheels" model enhances the solution's flexibility, enabling its use even when waste heat sources and end users are not physically connected to district heating infrastructure.

Table of Contents

List of figures

List of tables

Nomenclature

Abbreviations

AC	Active cooling
CHP	Combined heat and power
DC	Data centre
DHN	District heating network
FC	Free cooling
HoW	Heat on wheels
HTHP	High-temperature heat pump
ICE	Internal combustion engine
M-TES	Mobile thermal energy storage
NG	Natural gas
PCM	Phase change material
TCM	Thermochemical material
TCS	Thermochemical storage
TES	Thermal energy storage
VCRC	Vapour compression refrigeration cycle
WHR	Waste heat recovery

Thermodynamics

		Units
ΔP	Pressure drops in heat exchangers	$[Pa]$
COP	Coefficient of performance	[-]
EER	Energy efficiency ratio	[-]
$EER_{II,AC}$	Data centre air conditioning system second law efficiency	[-]
EER_{id}	Reverse Carnot cycle energy efficiency ratio	[-]
ε_{HEX}	Heat exchangers effectiveness	[-]
η_{fan}	Fan efficiency	[-]
m	Mass	$[kg]$
$\dot{m}_{DC}$	Supply air mass flow rate for DC cooling	$[kg/s]$
$\dot{Q}_{DC,cold}$	Data centre required cooling power	$[kW]$
$\dot{Q}_{DHN}$	District heating network thermal power demand	$[kW]$
Q_{sink}	Total heat rejected into the environment by DC cooling system	$[kWh]$
T_{amb}	Ambient temperature	$[°C]$
T_{charge}	TCM charging temperature	$[°C]$
$T_{DC,in}$	Supply cold air to the IT equipment	$[°C]$
$T_{DC,out}$	Return hot air from the IT equipment	$[°C]$
$T_{discharge}$	TCM discharging temperature	$[°C]$
$T_{Ext,in}$	Temperature of the external air entering the air-cooled condenser	$[°C]$
$T_{Ext,out}$	Temperature of the external air exiting the air-cooled condenser	$[°C]$
$T_{free\ cooling}$	Set-point temperature for Free Cooling mode	$[°C]$
T_H	Refrigerant condensation temperature	$[°C]$
T_L	Refrigerant evaporation temperature	$[°C]$
$T_{melting}$	Phase change temperature	$[°C]$
T_{return}	Temperature of the return line of the DHN	$[°C]$
T_{supply}	Temperature of the supply line of the DHN	$[°C]$

1. THUNDER concept

1.1. Introduction

D1.3 builds upon the analyses and results of D1.2, which should be consulted for a more complete understanding of the foundational elements on which the reference model for the energy system is based.

The THUNDER project aims to develop a strategy for utilizing thermal energy storage (TES) systems to improve the energy efficiency, economic feasibility, and environmental sustainability of recovering waste heat from data centres and reusing it in urban district heating networks.

During the early phases of the project, when analysing existing conditions, current practices and state-of-the-art technologies, a potential extension of the project scope emerged. This involved exploring configurations where heat recovery sources, storage systems, and energy reuse solutions are not necessarily physically interconnected via a direct hydraulic link. Instead, the "Heat on Wheels" approach was introduced, using mobile storage systems to connect energy sources and consumers that are geographically distant.

In Task 1.1.2, the THUNDER Concept, based on the integration of seasonal thermal storage and a thermal upgrade system, was examined alongside a set of connection strategies involving the waste heat recovery point, the thermal upgrade and storage systems, and the final point of reuse. These strategies were designed around the "Heat on Wheels" concept.

The solution developed for the THUNDER project combines seasonal thermal storage and thermal upgrade technologies with a mobile storage and transport system using Phase Change Materials (PCMs). PCM based systems offer a high level of technological maturity, a wide range of phase change temperature options to match various thermal requirements, suitability for road transport, and safe operation, particularly in urban environments.

The introduction of this mobile storage solution necessitates new design and prototyping activities (covered in WP2) to develop a PCM based thermal storage device. This prototype will be tested and later implemented in the Varna demonstrator.

Task 1.1.2 also involved the development of a numerical simulation tool for modelling the complete energy chain. This tool, built using Python, supports the development of various project functions such as control logic and monitoring. It models and characterizes each component of the THUNDER energy system and its interconnections. The tool was used to simulate the demonstrator configuration as well as alternative scenarios to assess the replicability of the system in different contexts.

Specifically, the scenarios retained constant parameters for the waste heat source (steady power and temperature) and the thermal user (a district heating network similar to the demonstrator's one).

D1.3 shows that a seasonal thermal storage system based on innovative low temperature thermochemical materials, when integrated with a high-performance thermal upgrade system, can significantly improve the energy, economic, and environmental sustainability of waste heat recovery and reuse in urban areas. Moreover, the "Heat on Wheels" model enhances the solution's flexibility, enabling its use even when waste heat sources and end users are not physically connected to district heating infrastructure.

1.2. Advances of the THUNDER concept design

Figure 1 represents the scheme of the THUNDER concept design proposed in D1.2: the use of seasonal mobile TES (M-TES) allows connecting waste heat (WH) sources (data centre (DC)) and waste heat recovery (WHR) sinks (DHN)) separated by distances that cannot be coupled cost effectively with a piping network.

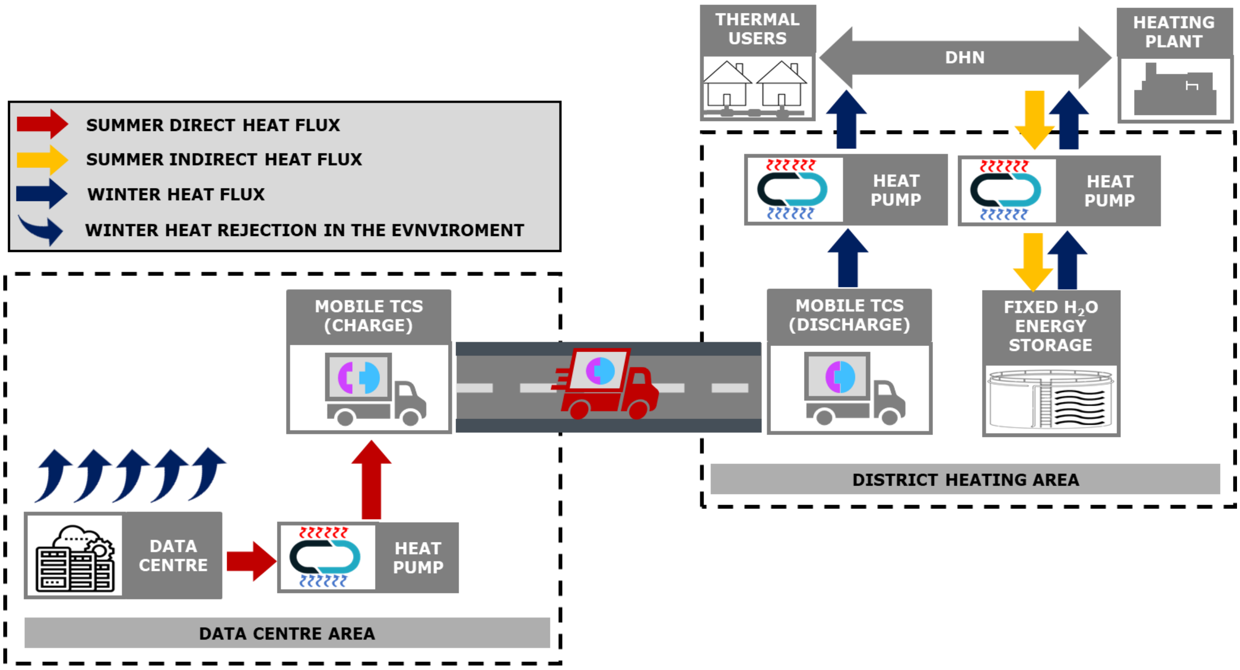

Figure 1: THUNDER's first conceptual design

This configuration presented some issues that necessitated a slight reassessment of the initial design. The primary concerns leading to this revision were related to safety, space constraints, and weight limitations. In particular, after careful recognition of the space hosting the case study, it has been noted that the presence of the equipment necessary for the Thermochemical Storage (TCS) would have posed some problems of proper management of temperature and pressure levels of the technical fluids. In this sense, the decoupling between the heat source (data centre waste heat) and TCS would have been beneficial. The new proposed design not only solves these issues but also introduces beneficial aspects.

When using Thermochemical Material (TCM) as a "Heat on Wheels" (HoW) solution, the system would require water temperatures ranging to 100°C, as the TCM charging process occurs near this threshold. Consequently, pressurized piping would be necessary, introducing stricter safety regulations compared to systems operating at the usual temperature of DC Cooling condensing (around 60°C with higher values).

Another factor promoting a redesign was the possible noise generated by the air flow rates required for TCM charging. This poses a significant issue since the data centre is located in a residential area, where interaction with non-technical personnel is frequent.

Additionally, the DC is part of a larger building, meaning the available space for TCM storage is limited, and the maximum weight must remain within transport constraints (i.e., requiring a truck with an integrated crane). These restrictions make the use of mobile TCM storage highly challenging.

1.3. Varna concept design

Given these constraints, the decision was made to implement Phase Change Material (PCM) for the HoW solution. This approach employs consolidated and reliable technology, overcoming the issues born after the recognition of the hosting space.

While TCS offers notable technological advantages, its innovative nature introduces operational complexities, particularly in mobile applications. As a result, the TCS system has been relocated to Veolia's facility, into the DHN area, where it operates as a fixed installation rather than a mobile unit. This adjustment resolves all the challenges previously outlined:

- High charging temperatures (around 100°C), which could be used in the charging phase, are no longer a safety concern as the system is now housed in an industrial environment with trained personnel.
- Noise from high airflow rates, space constraints, and weight limitations is mitigated, as industrial zones are less sensitive to these factors and are equipped to handle them.
- The requirement for a continuous TCM charging process is addressed by decoupling the system from the data centre cooling needs. Indeed, the PCM based storage (which does not require an uninterrupted charging process) is now directly integrated with the DC cooling system that can operate in its proper manner, recovering waste heat when it is beneficial. This ensures the cooling system can respond dynamically to the data centre's load demands, without being constrained by TCM charging cycles.

When discharging the PCM into the TCS system, the high temperature heat pump will operate solely based on the TCM's charging needs, as PCM discharge does not impose strict limitations.

The proposed new configuration is illustrated in Figure 2.

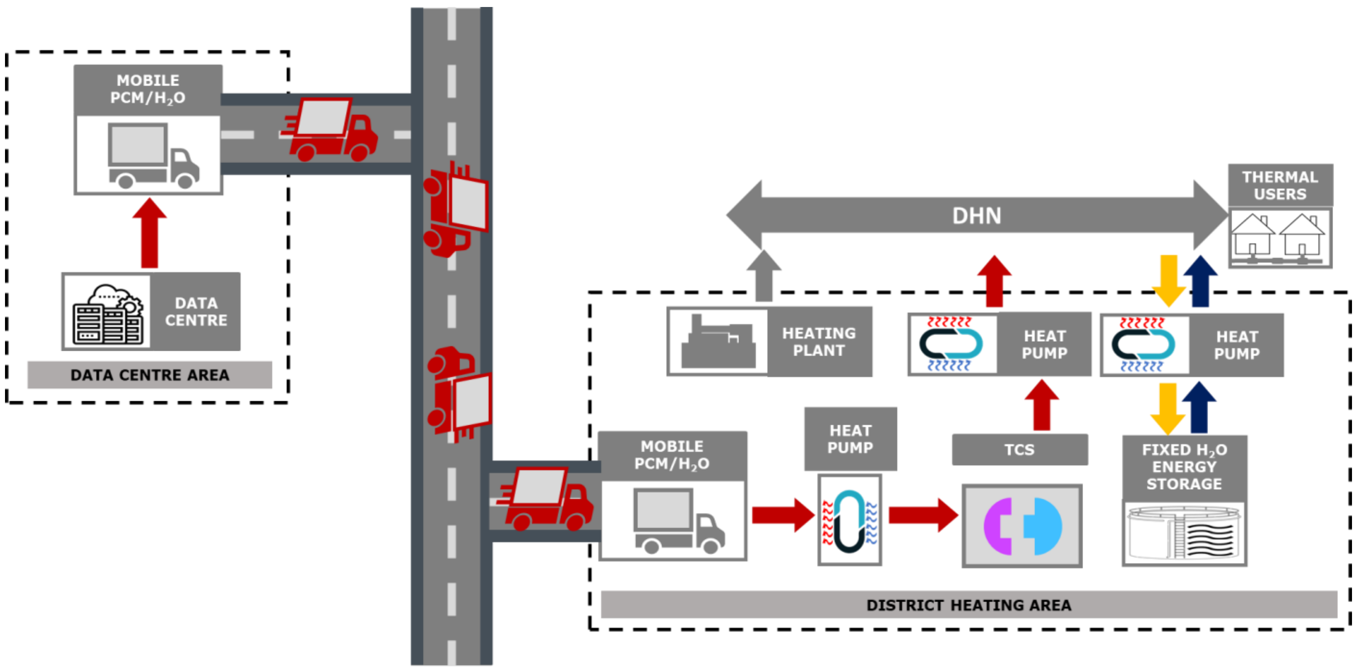

Figure 2: THUNDER Varna conceptual design

1.4. Numerical simulation tool

To obtain the results presented in this study, a comprehensive simulation tool has been developed in a Python environment. This computational model was designed to replicate the behaviour of the integrated system, including all key components: the data centre (DC), high temperature heat pump (HTHP), phase change material (PCM) mobile storage, thermochemical material (TCM) storage, and district heating network (DHN).

For all the tools presented below, an hourly time step has been adopted in the temporal simulation of the various models. This approach ensures seamless integration and communication between the different components, avoiding issues related to inconsistent temporal discretisation across the models.

1.4.1. DC numerical tool

In Figure 3, the main parameters for the tool used to simulate the data centre operation are presented.

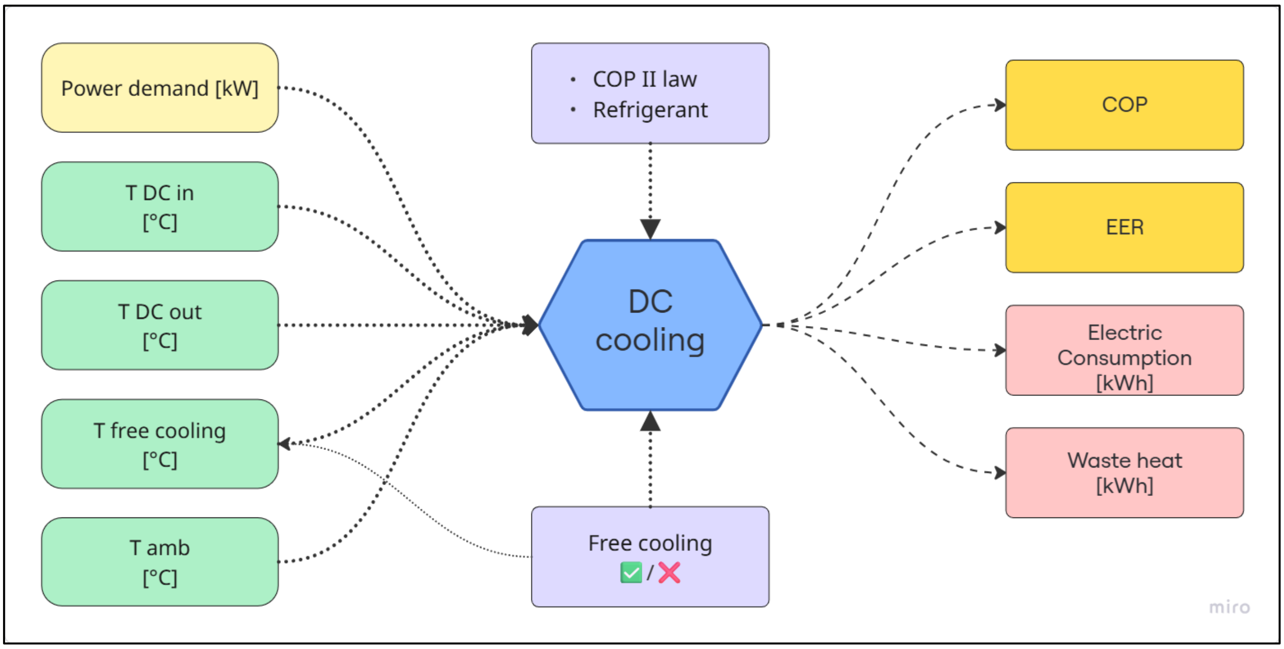

Figure 3: DC simulation tool, main parameters

On the left side of Figure 3, the required inputs are shown, such as the annual cooling demand profile, the inlet and outlet water temperatures, referred to as $T_{DC,in}$ and $T_{DC,out}$ in Figure 12. Another essential input is the ambient temperature profile of the location where the data centre is located. This value is necessary to determine the condensation temperature required by the chiller to ensure heat rejection from the rack area to the environment. If free cooling is available, it is also needed to set the threshold temperature below which it can be activated.

In the central section, two additional key parameters are displayed, which are fundamental for simulating the chiller cycle. It is necessary to specify the refrigerant used to retrieve its thermophysical properties. Another required input is the second law efficiency of the chiller. This enables a performance analysis based solely on operating temperatures, rather than relying on fixed Coefficient of Performance (COP) values associated with specific commercial units. A more detailed discussion of this assumption is provided in D 1.2.

On the right side, the output generated by the simulation tool is reported. These include the COP value and, consequently, the chiller's Energy Efficiency Ratio (EER), as well as its annual energy consumption, broken down by individual components of the cooling system and the total system consumption. If free cooling is employed, the results will also be split between free cooling and active cooling modes. The amount of waste heat discharged from the chiller condenser to the environment is also calculated. In the case of free cooling, this heat is further divided between the two modes. This distinction is important, as the heat rejected via free cooling occurs at a lower temperature compared to active cooling, making the latter more suitable for potential heat recovery applications.

1.4.2. DHN numerical tool

In Figure 4, the main parameters related to the DHN simulation tool are presented.

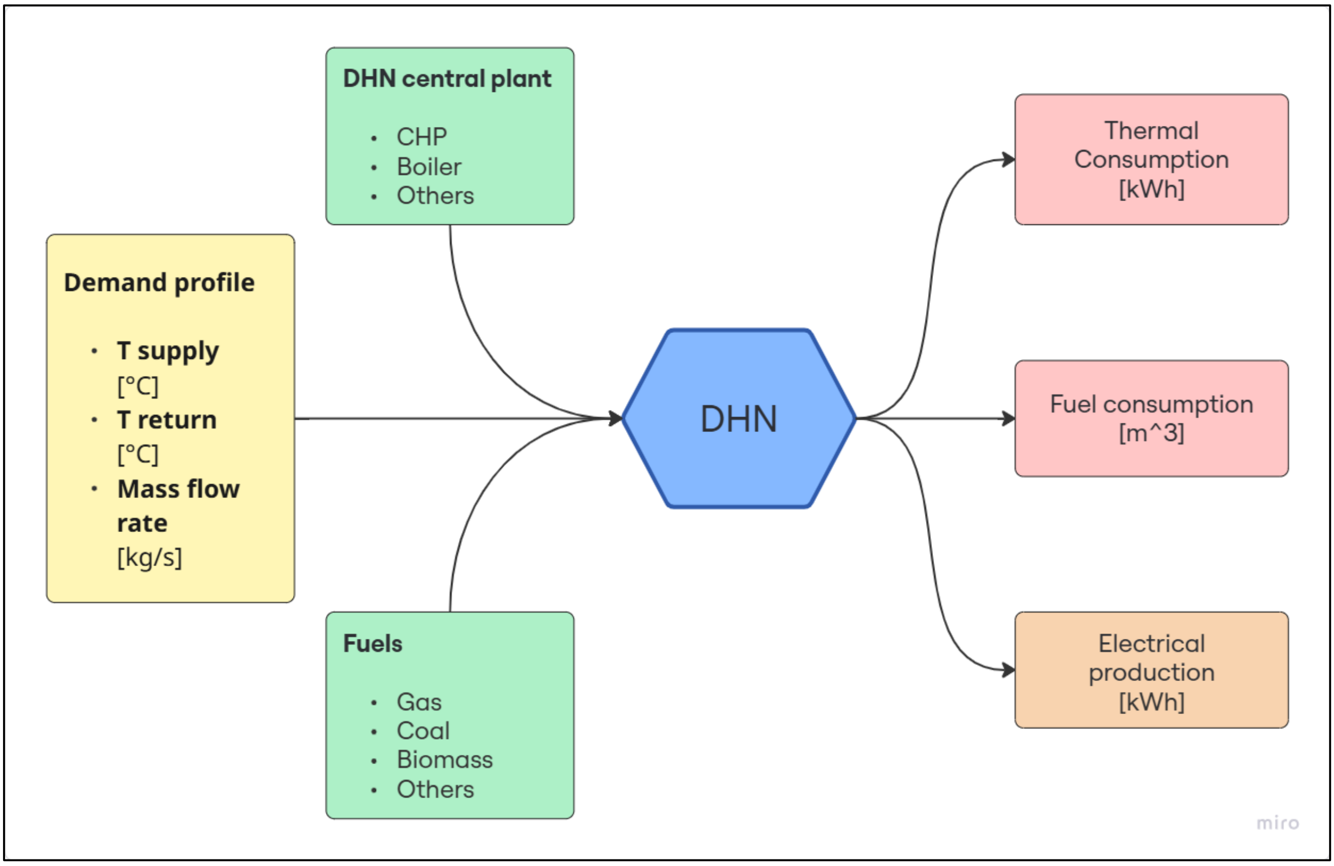

Figure 4: DHN simulation tool, main parameters

The tool developed for simulating the performance of a DHN takes as input the annual operational hourly profile of the selected network. The required input values include the T_{supply} and T_{return} temperatures, the network's mass flow rate, the type of thermal plant, and the type of fuel used.

Once these values are provided, the model replicates the thermal demand profile of the network on an hourly basis. As output, the tool provides the total thermal demand from the users, the fuel consumption, and, if a cogeneration system is employed, the estimated electricity production.

1.4.3. HTHP numerical tool

In Figure 5, the main parameters related to the HTHP (High temperature heat pump) simulation tool are presented.

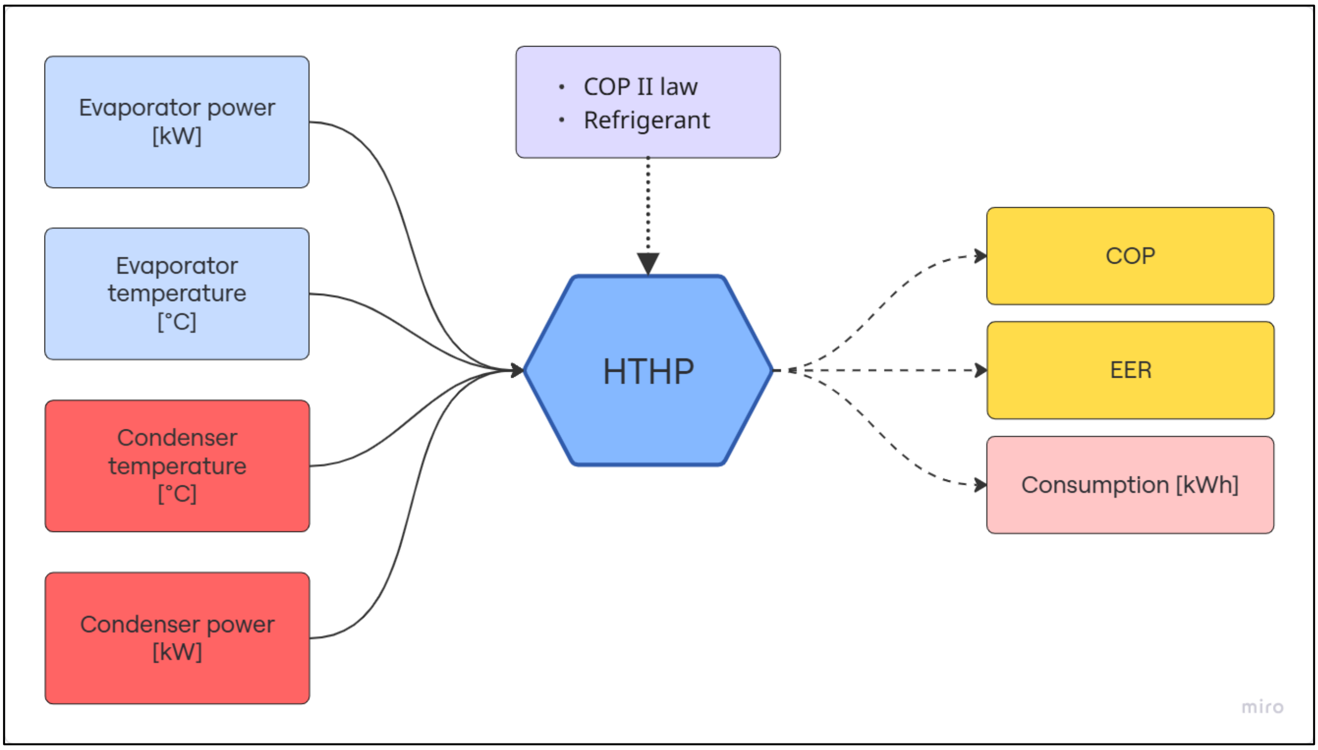

Figure 5: HTHP simulation tool, main parameters

This tool enables the simulation of a HTHP. The required inputs include the operating temperatures at the evaporator and condenser, which depend on the specific application scenario of the heat pump. Additionally, the thermal powers at the evaporator and condenser are provided as inputs. This allows the numerical model to analyse different heat pump sizes. Depending on the case study, it is necessary to satisfy either the evaporator or condenser thermal demand; once one of the two powers is fixed along with the operating temperatures, the other is calculated as an output.

Another required input is the type of refrigerant used, so that its thermophysical properties can be considered. As in the case presented in 1.5.2, a second law efficiency value is also assigned, enabling the calculation of the COP and, consequently, the EER. Operational performance data for HTHP have been estimated and will be validated in Task 2.1 of WP2.

The main output of the model is the electrical consumption of the heat pump required to meet the specified thermal demands.

1.4.4. TCM seasonal storage system numerical tool

In Figure 6, the main parameters related to the TCM seasonal storage simulation tool are presented.

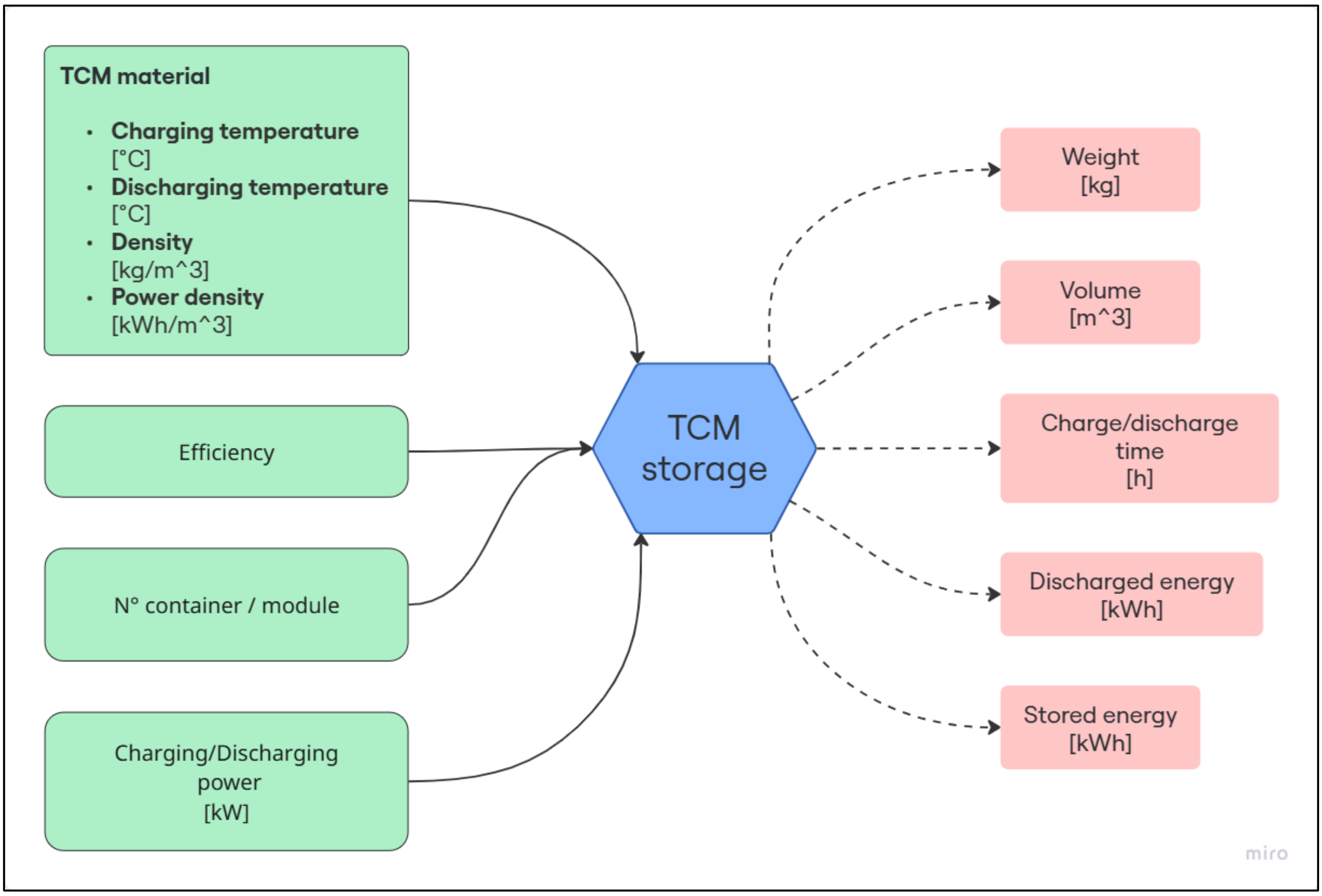

Figure 6: TCM storage simulation tool, main parameters

This model simulates the operation of a seasonal thermal energy storage system based on TCM. The data have been estimated using reference values from Task 2.2 of WP2. Experimental tests and a demonstrator pilot will validate them. The required inputs include the characteristics of the TCM, specifically the charging and discharging temperatures, which define the thermal boundaries of the system. Additionally, the material density and energy density must be provided. The former is used to calculate the occupied volume based on the required mass, or vice versa. In scenarios where spatial constraints exist, the maximum allowable volume is defined first, and the corresponding mass is then derived.

An efficiency value must also be specified. At this stage of TCM research, where the technology is still emerging and not yet fully characterised, this efficiency accounts for various losses: during charging, discharging, storage process and other potential inefficiencies. While the long-term goal is to achieve unitary efficiency, a conservative value of 0.8 is currently adopted.

Other required inputs include the charging and discharging power levels, which are dictated by the components supplying or demanding heat during the respective phases. The number of containers or modules must also be specified. This modular approach allows for optimised management of the charging and discharging processes across individual units, while still providing a total system-level thermal storage capacity. The modularity of the storage system is a key feature, as it significantly broadens the range of potential applications.

The model outputs include both physical characteristics, such as total and per-module volume and weight, and energy related metrics, including the total stored energy, the energy released, and the duration of the charging and discharging phases. The power profile during these phases can be either constant or time-varying.

1.4.5. PCM storage system numerical tool

In Figure 7, the main parameters related to the TCM seasonal storage simulation tool are presented.

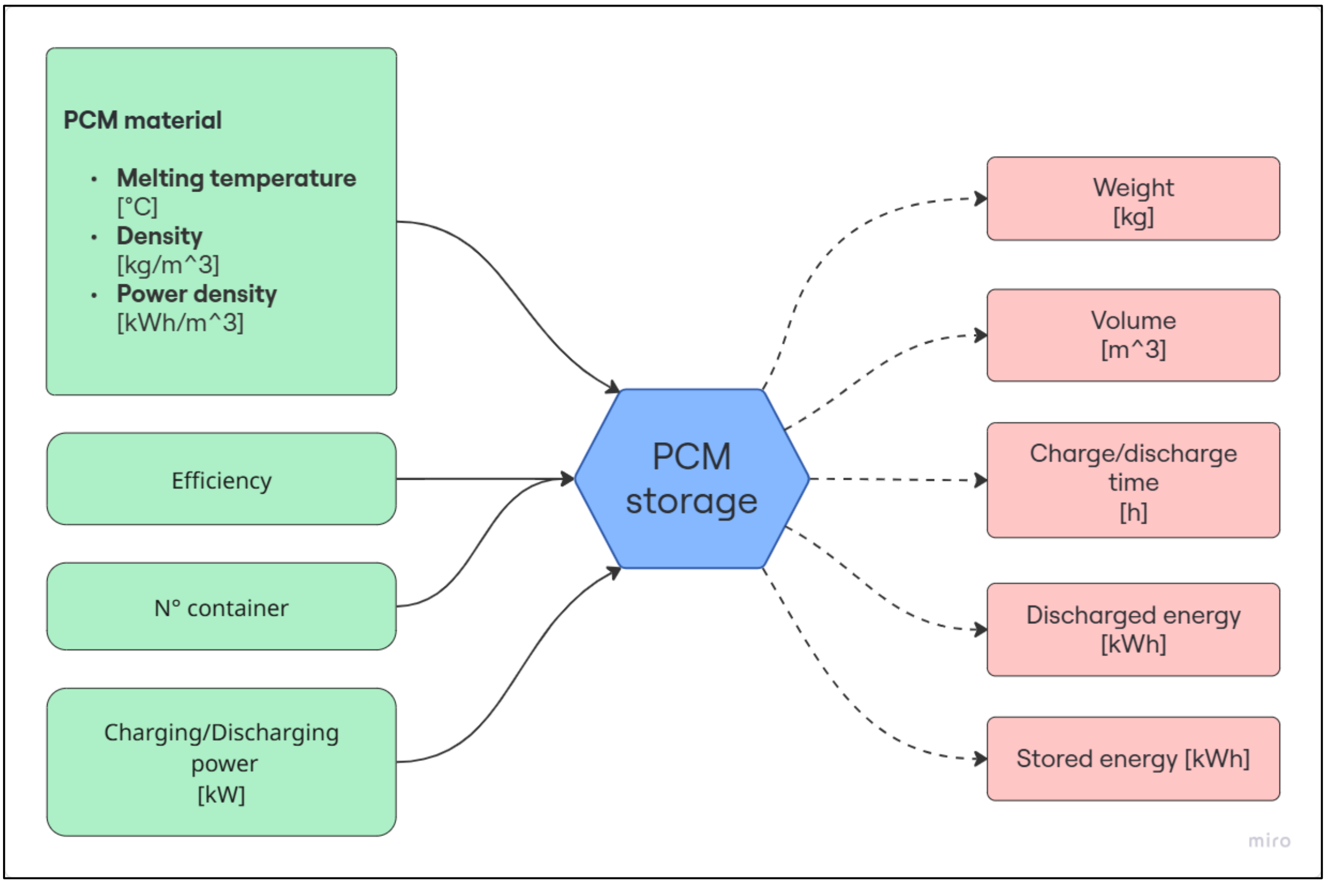

Figure 7: PCM storage simulation tool, main parameters

The tool that models TES using PCM operates in a manner largely analogous to the TCM-based storage system described in 1.4.4. The main differences between the two systems lie in the charging and discharging temperatures, which in the case of PCM coincide and are defined by the material's phase change temperature.

For PCM systems, it is necessary to define an efficiency value that accounts for thermal losses to the environment. This efficiency should ideally be calculated based on the heat exchange with the ambient air through the storage materials and the insulation used. However, since the current model is in a preliminary stage and aims to provide a high-level overview of the overall energy chain, a constant efficiency value is assumed. This value is selected based on the duration of heat storage and the temperature at which the heat is stored in the PCM system.

1.5. Varna's demonstrator

This section presents the results of the simulation code when applied to a power system such as the one that will be realized at the Varna demonstrator. Initially, the characteristics and energy consumption of the Abilix DC located on site, as well as those of the Veolia DHN, will be presented.

This report provides the main information; for a more comprehensive and in-depth analysis, refer to D1.2, which describes the state of the art of the technologies implemented in the demonstrator, as well as detailed results on the operation of both the DC and the DHN.

1.5.1. DHN's results without waste heat integration

The core of Veolia Energy Varna's system is a sophisticated DHN that combines high efficiency cogeneration (CHP) units with modern boilers. The company operates five CHP units, fuelled by natural gas (NG), providing a total thermal power of 11.2 MWth and an electrical power of 11.05 MWel; the technical characteristics of internal combustion engines (ICEs) for CHP operation are shown in Table 1. Complementing the CHP units, the system includes three hot water boilers manufactured in Bulgaria: the first boiler has a rated thermal power of 20 MWth, whereas the remaining two have a rated thermal power of 7.5 MWth. These boilers use NG as fuel and can modulate their power in winter months from 15% to 100%, providing crucial operational flexibility to adapt to fluctuations in energy demand.

ICE number	Thermal rated power [MW_{th}]	Electrical rated power [MW_{el}]
1	2.41	2.43
2	2.44	2.38
3	2.44	2.41
4	2.41	2.43
5	1.5	1.4

Table 1: Technical characteristics of ICES's installed in Veolia's thermal plant in Varna

The network is driven by two main pumps that ensure efficient heat distribution: one is a high-capacity pump with a nominal flow of 1400 m^3/h, and the other has a nominal flow of 1200 m^3/h, both operating with an inverter.

The system operates in two main modes, adapting to the city's seasonal needs: during the heating season (November 1 to April 30), all CHP units operate at full power to meet high demand. Boilers operate flexibly, adjusting according to the outdoor temperature. Total thermal load ranges between 12 and 30 MW_{th}, depending on weather conditions, while total electrical load remains constant at 11 MW_{el}. Supply/return temperatures vary between 90/70 °C and 70/50 °C, adjusting to the outdoor temperature to optimize efficiency.

In the Summer Season (April 30 to November 1), CHP units operate at reduced capacity, with an average of 5 MW of electrical and thermal power. Supply/return temperatures are maintained between 80/60 °C and 70/50 °C.

The operations of Veolia Energy Varna equipment are regulated by an advanced SCADA (Supervisory Control and Data Acquisition) system. This system is supervised 24 hours a day, 7 days a week by a team of highly trained engineers. The SCADA system allows real time power adjustment based on outdoor temperature and network demand, monitoring and optimizing the efficiency of each system component, quickly detecting and responding to any anomalies or inefficiencies, and collecting detailed data for analysis and continuous improvement of operations.

Currently, Veolia Energy Varna supplies hot water and heating to over 10 000 customers, encompassing a wide range of users. These include residential homes, which constitute the majority of the customers, local businesses and commerce, municipal and administrative buildings, and public institutions such as schools and hospitals.

This tool allows the replication of measured data (provided by the DHN operator) for the thermal powers required by the network, subdivided between ICEs and boilers coverages, as shown in Figure 8. Annually, the global DHN thermal energy demand amounts to 81 161 MWh_{th}/year, covered for 81.5% by the ICEs, while the remaining 18.5% is supplied by the boilers.

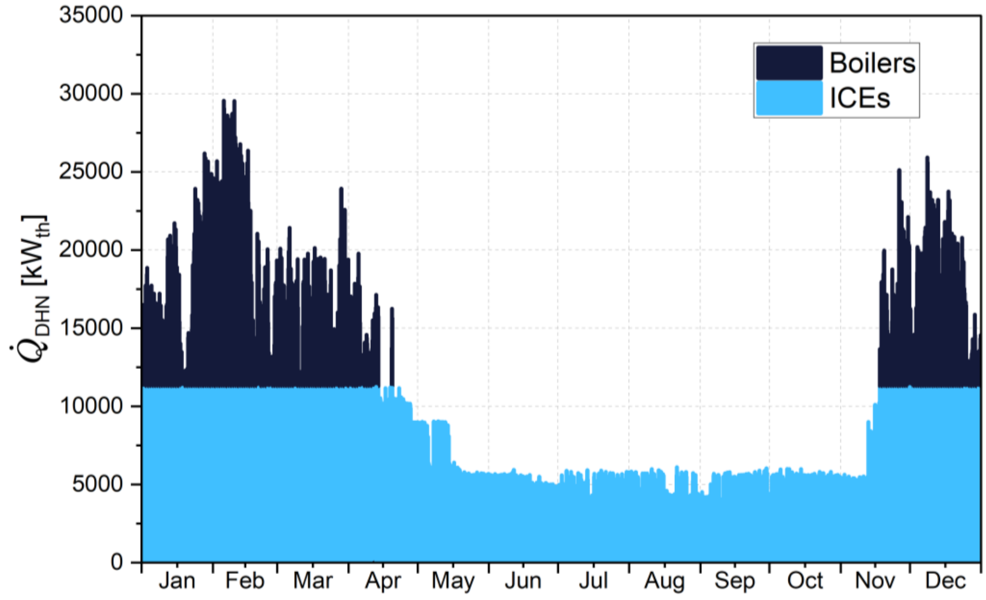

Figure 8: Hourly DHN thermal power demand coverages of the boilers and the ICEs

1.5.2. DC's results without waste heat recovery

The Abilix DC is equipped with dual electricity grid connections, always ensuring an uninterrupted power supply. The facility houses distinct power groups, contributing to its high operational resilience. To further safeguard against power disruptions, Abilix has implemented an N+1 redundant Uninterruptible Power Supply (UPS) system. The redundant UPS configuration ensures that clients experience seamless service, even during unexpected power outages.

The DC is equipped with over 30 racks, each meticulously managed to offer optimal performance and security.

With a total installed power capacity exceeding 150 kW_{el}, the DC currently load is 16.55 kW_{el} (average value) of IT equipment (most of the equipment does not consume peak power). Based on measured electrical power data, no seasonal trend can be identified (Figure 9). The same trend is shown in Figure 10: the IT-electrical power input is fairly constant during the day. Only a weekly trend exists, related to the weekend lower data traffic (Figure 11).

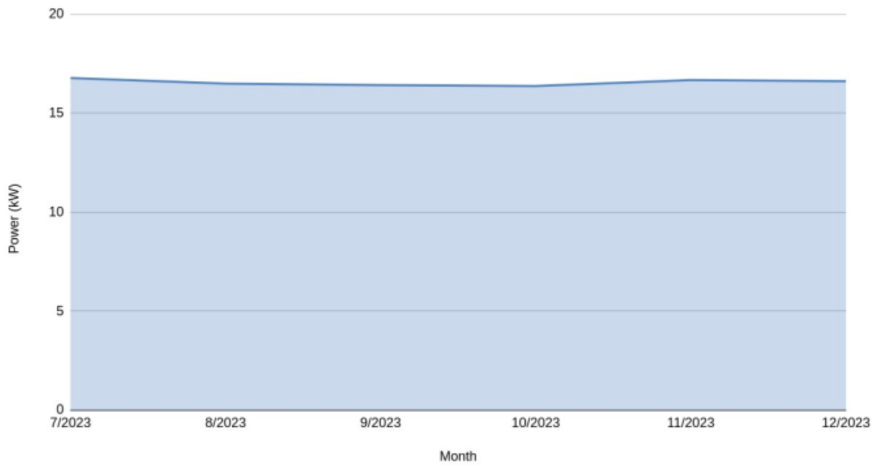

Figure 9: Abilix's IT equipment measured power absorption at different months

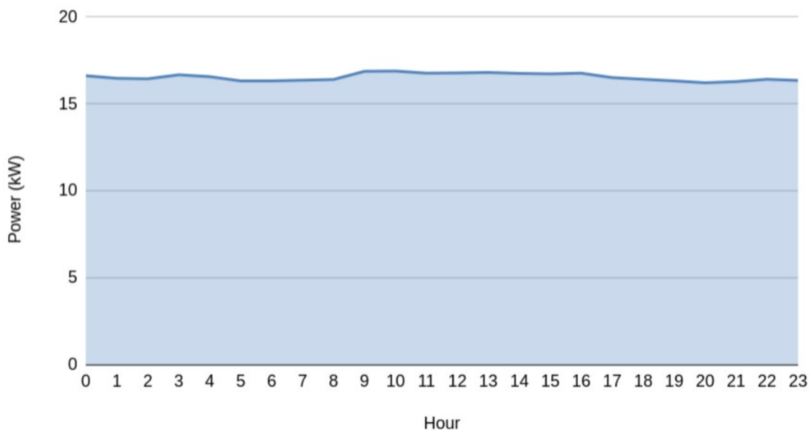

Figure 10: Abilix's IT equipment measured power absorption at different hours

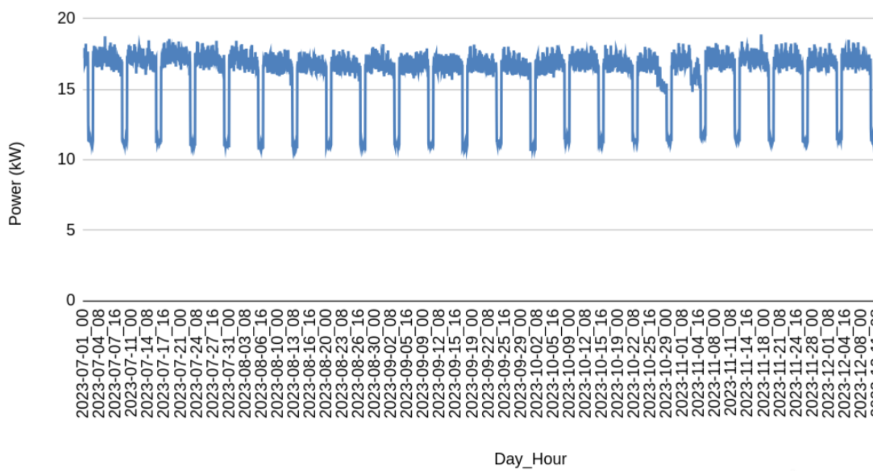

Figure 11: Abilix's IT equipment measured power absorption on days of the week, including weekends

The cooling system installed is a group of redundant direct expansion air conditioning units based on hot/cold aisle containment which cool a 30-37°C air stream from the hot sides of the racks to an inlet operative temperature of 22-25°C. The rated cooling power is 14 kW_{th} (3.5 to 16 kW_{th}) per unit with an electrical power consumption of a single unit of up to 4.22 kW_{el}. The AC group is capable of providing up to 64 kW_{th} of cooling power.

The cooling system of Abilix's DC operates exclusively with active cooling, referred to here as air conditioning (AC) mode, as illustrated in Figure 12.

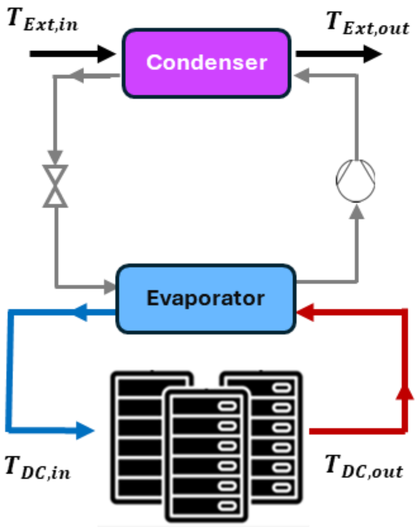

Figure 12: DC active cooling similar to the one in Abilix DC

As commonly assumed, the cooling power needed for the IT equipment is equal to the electrical power used for its operation, as all electrical power is considered to be dissipated as heat. According to Abilix, the cooling power demand remains relatively constant, with no significant seasonal or hourly fluctuations, aside from a slight reduction during weekends. Therefore, for this preliminary energy model, the cooling power required by the DC ($\dot{Q}_{DC,cold}$) is assumed to be constant throughout the year, set at approximately 15 kW_{th}.

The vapour compression refrigeration cycle (VCRC), therefore, manages that cooling load at the evaporator side, rejecting the heat into the environment at the condenser side through an electric energy consumption connected to the compressor operation, which increases the working fluid pressure to the level required for the condensation process. To calculate the compressor power consumption ($\dot{W}_{comp,AC}$), it is necessary to estimate the EER of the cycle: this has been simply done by imposing the efficiency in terms of Thermodynamics Second Law (value set constant at 0.5, as a first approach), calculated in accordance with the equation (1) as the ratio between the actual value and the ideal value given by a reverse reference (ideal) cycle that operates between the same source and sink.

(1)

$$EER_{II,AC} = \frac{EER}{EER_{id}} = \frac{EER}{\frac{T_L}{T_H - T_L}}$$

where T_L and T_H are the low and high saturation temperatures of the refrigerant of the VCRC, in this simplified energy model. It is worth noting that the EER_{id} has been evaluated considering the refrigerant sides, even the source sides, which vary their temperature during refrigerant evaporation and condensation.

This cooling system is strictly essential during the summer months when the external air temperature is high. In contrast, during the winter months, the external air temperature can drop below the working fluid evaporation temperature. To ensure the operation of the VCRC, a minimum temperature lift of 10 K must be maintained, as the condensation temperature in the reverse cycle cannot be lower than the evaporation temperature.

Given the relationship between the *EER* and ambient temperature, it is possible to calculate the power consumption of the compressor and the heat rejected to the environment using equations (2) and (3), respectively.

(2)

$$EER = \frac{\dot{Q}_{DC,cold}}{\dot{W}_{comp,AC}}$$

(3)

$$\dot{Q}_{sink} = \dot{Q}_{DC,cold} + \dot{W}_{comp,AC}$$

The energy model accounts for the contributions of the fans used to move cooling air ($\dot{m}_{DC}$) at the indoor terminal unit and external air ($\dot{m}_{Ext}$) at the outdoor terminal unit. These contributions are included in total energy consumption, in addition to that of the compressor.

Equation (4) can be used to calculate the airflow rate of cooling air that must be continuously provided to the DC ($\dot{m}_{DC}$); $\dot{Q}_{DC,cold}$ is the cooling power that the cooling system must provide to the servers, while $T_{DC,in}$ and $T_{DC,out}$ are the supply of fresh air and the hot air returning from IT equipment, respectively.

(4)

$$\dot{Q}_{DC,cold} = \dot{m}_{DC} \cdot c_{p,air} \cdot (T_{DC,out} - T_{DC,in})$$

The external airflow rate is determined by equation (5) where $\dot{Q}_{sink}$ is the thermal power at the condenser evaluated at the working fluid side through equation (8) while $T_{Ext,in}$ and $T_{Ext,out}$ are the temperatures related to the external air flow rate as depicted in Figure 12.

(5)

$$\dot{Q}_{sink} = \dot{m}_{Ext} \cdot c_{p,air} \cdot (T_{Ext,out} - T_{Ext,in})$$

The temperature of the external air entering the condenser($T_{Ext,in}$) has been set equal to the ambient temperature; since the case study pertains to the city of Varna (Bulgaria), the meteorological data for outdoor temperature has been considered for the specific location [1]. The temperature of the external air exiting the condenser is assumed to be equal to the working fluid condensing one (T_H).

Given the known airflows, both on the DC side and the outdoor side, it is possible to calculate the power consumption of the fans using equation (6) and determine the corresponding annual energy consumption, assuming proper pressure drop on the heat exchanger and fan efficiency. All the imposed conditions for the regulations of AC mode are summarised in Table 2 in which the temperature of the air returning from the DC ($T_{DC,out}$) is set according to indications of technical-scientific literature to ensure IT equipment reliability [2] and the data provided by Abilix.

$$W_{fan} = \frac{\dot{m} \cdot \Delta P}{\rho_{air} \cdot \eta_{fan}} \tag{6}$$

Thermodynamic variables	Abbreviations	Units	Imposed values
Required cooling power	$\dot{Q}_{DC,cold}$	[kW]	15
Supply cold air to the IT equipment	$T_{DC,in}$	[°C]	20
Return hot air from the IT equipment	$T_{DC,out}$	[°C]	35
Pressure drops in heat exchangers	ΔP	[Pa]	150
Fan efficiency	η_{fan}	[-]	0.6
Second law efficiency	$EER_{II,AC}$	[-]	0.5

Table 2: Imposed conditions for the regulations of AC mode

The whole AC system is responsible for an annual electricity consumption of 14.9 MWh/y; the compressor electricity absorption ($\dot{W}_{comp,AC}$) is 10.2 MWh/y, while the energy consumption associated with the fans' operation is 4.8 MWh/y. The trend of the related power absorption over the year is shown in Figure 13.

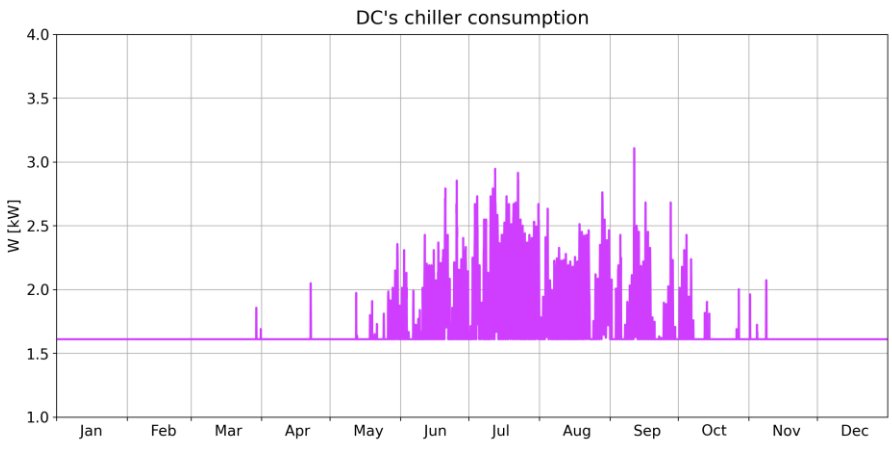

Figure 13: DC's annual chiller consumption profile

The chiller's COP ranges from a maximum value of 14.90 (achieved at the minimum 10°C lift between evaporator and condenser) to a minimum of 6.89 (occurring when outdoor temperature peaks at 32.55°C). Figure 14 presents the corresponding waste heat profile from the DC chiller's condenser.

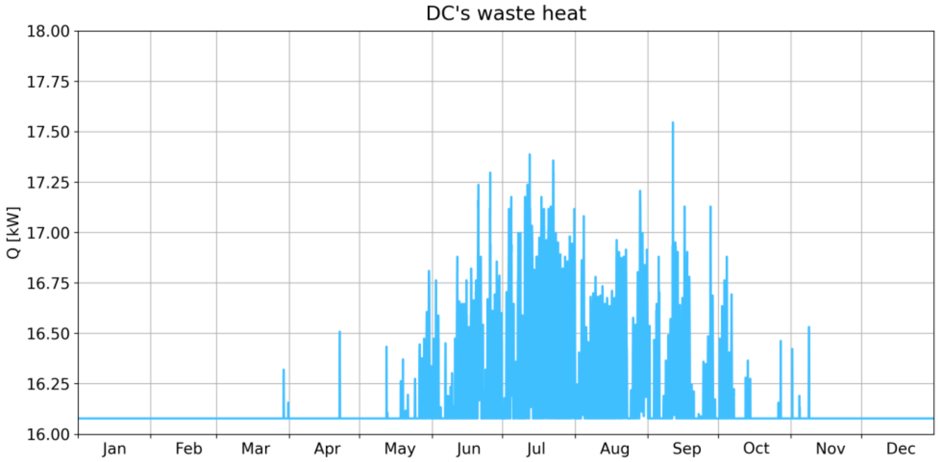

Figure 14: DC's waste heat profile

1.5.3. TCM storage system

In the THUNDER project, the selection of materials to be tested focuses on composite materials consisting of salts combined with a host matrix, as these represent one of the most promising solutions in the field of thermochemical storage due to the extensive research dedicated to their development and optimisation. A careful literature review has been conducted, with a specific focus on energy densities and hydration/dehydration temperatures suitable for the project's experimental activities. The list of the selected salts with some working parameters is indicated in Table 3.

Salt	Energy density [GJ/m³]	Hydration temperature [°C]	Dehydration temperature [°C]
$CaBr_2$	2.67	74	81
$CaCl_2$	3.10	32	71
K_2CO_3	1.56	62	69
$SrBr_2$	1.99	48	54

Table 3: Selected TCM with relevant properties

Choosing an appropriate host matrix is equally crucial, as it must not only retain the salt and prevent its dispersion but also offer porosity to enhance energy and mass transfer, prevent deliquescence during hydration, and strike a balance between the availability of free pores after salt impregnation and optimal transfer efficiency [3]. The selected host materials—vermiculite [3–5], zeolite [6,7], and silica gel[8,9]—were chosen based on demonstrated performance, commercial availability, and cost-effectiveness. Since TCMs are not yet commercially available, and composites made from hydrated salts in porous matrices are also absent from the market, only a few specialised companies can produce them in limited quantities, mainly for high temperature applications. PCM Products, a partner in the THUNDER consortium, operates in this niche sector and contributes to the project by identifying suitable materials for the creation of TCMs tailored to the project's operational needs, producing composites by combining salts such as $LiCl_2$, $MgCl_2$, $CaCl_2$, LiBr, and NaOH with absorbent materials like perlite, vermiculite, and graphite, uniformly mixing them, dehydrating the mixture, and sealing the final composite in vacuum bags to preserve its properties until use. The company has compiled a list of composite materials (Table 4).

Thermo Chemical Material	TCM-81	TCM-71	TCM-65	TCM-110	TCM-72	TCM-127	TCM-113	TCM-28	TCM-122	TCM-250
Energy Capacity (lit) (GJ/m3)[a]	2.67	3.10	1.30	2.03	2.22	2.48	2.29	2.27	2.49	-
Dehydration Temp (deg C)[a]	**81**	**71**	**65**	**110**	**72**	**127**	**113**	**28**	**122**	**>150[d]**
Dehydration Mechanism [a]	6 → 0	6 → 0	1.5 → 0	2 → 0	3 → 0	6 → 1	6 → 0	7 → 1	6 → 0	-
Density (hydrate)	2.0	1.5	2.0	1.6	1.5	1.5	1.5	1.7	2.4	-
Density (anhyd)	3.35	2.15	2.43	3.46	2.07	2.32	2.30	2.66	4.22	
Energy Capacity per kg (kJ/kg)[c]	797	1442	535	587	1072	1069	996	853	590	480[b]
Salt loading on absorbent (as anhyd) (%)[d]	73.5	68	62	70	57	40	54	46	67	-
Bulk Density of salt/absorbent TCM (dry)[d]	0.375	0.221	0.215	0.307	0.217	0.221	0.249	0.200	0.297	0.64
Energy Density (kJ/l)[e]	**220**	**217**	**71**	**126**	**133**	**94**	**134**	**78**	**117**	**307**
Energy Density (kWh/m3)	**61**	**60**	**20**	**35**	**37**	**26**	**37**	**22**	**33**	**85**
Energy Density (RT-h/USG)	**0.066**	**0.065**	**0.021**	**0.038**	**0.040**	**0.028**	**0.040**	**0.023**	**0.035**	**0.092**
Energy Density (Btu/USG)	**789**	**778**	**256**	**453**	**476**	**339**	**481**	**282**	**421**	**1102**

Table 4: TCMs characteristics. Notes: a = http://dx.doi.org/10.1016/j.apenergy.2017.04.080; b = http://dx.doi.org/10.1016/j.enconman.2017.03.080; c=energy capacity *(GJ/m3) / density; d = experimental data; e = (energy capacity (kJ/kg) x salt loading (%) x bulk density) / 100.*

The total volume of TCM contained within the storage unit at Veolia's premises is 10 m^3. The charging temperature is around 100°C, while the discharge temperature is set around 40°C, with an energy density of around 100 kWh/m^3. TCS efficiency is assumed to be 80%, meaning 80% of the stored energy is effectively released. This conservative assumption accounts for environmental heat losses, operational inefficiencies during charging/discharging, and other system performance factors. Table 5 shows a comparison between average sensible, latent and thermochemical storage systems, based on meaningful parameters for seasonal thermal storage.

	Sensible	**Latent**	**Chemical**
Capacity	10-50 kWh/ton	50-100 kWh/ton	120-150 kWh/ton
Power	0.001-10 MW	0.001-1 MW	0.01-1 MW
Efficiency	50-90%	75-90%	75-100%
Cost	0.1-10 €/kWh	10-50 €/kWh	8-100 €/kWh
Temperature range	Up to: 100°C (water tanks) 50°C (aquifers and ground storage)	20-40°C (paraffins) 30-80°C (salt hydrates)	20-200°C

	Sensible	Latent	Chemical
Storage density	Low: 55 kWh/m3	Moderate: 80 - 140 kWh/m^3	Normally high: 140 - 830 kWh/m3
Lifetime	Long	Often limited due to storage material cycling	Depends on the reactant degradation and side reactions
Technology status	Available commercially	Available commercially for some temperatures and materials	Generally, not available, but undergoing research and pilot project tests
Advantages	Low cost Reliable Simple application with available materials Simply systems	Medium storage density Small volumes Short-distance transport possibility	High storage density Low heat losses Long storage period Compact energy storage Long-distance transport possibility
Disadvantages	Significant heat loss over time Large volume needed	Low heat conductivity Corrosivity of materials Significant heat losses	High capital costs Technically complex

Table 5 Comparison of the three available technologies for seasonal thermal energy storage [10–12]

1.5.4. PCM Heat Recovery System

When the mobile PCM ("Heat on Wheels") storage system is implemented to recover WH and transport it to the fixed TCS near Veolia, the DC's chiller no longer condenses on the outdoor air.

The selection of the PCM was based on the need to optimise its integration both with the data centre's cooling system, where waste heat is recovered, and with the TES system, where the recovered heat is subsequently transferred for seasonal storage.

In terms of coupling with the DC, it is necessary to select a material with a relatively low melting temperature. A higher melting point would result in a significant drop in the efficiency of the chiller responsible for cooling the data centre, or in some cases, the compressor might not be able to bring the refrigerant to the required condensation temperature at all. Consequently, a PCM with a phase change temperature of approximately 48°C was selected.

This temperature allows for direct heat recovery by connecting the data centre's cooling loop to the PCM system. At this operating point, condensation occurs at around 60°C, resulting in a thermal lift of approximately 45°C for the compressor.

The main advantage of using a PCM lies in the ability to maintain nearly constant temperature conditions during both charging and discharging phases. This ensures optimal matching with the temperature levels involved.

As for the integration with TCS, a similar approach has been applied. A PCM with a phase change temperature of 48°C enables the use of a HTHP operating with a stable heat source temperature. This facilitates achieving the required thermal lift between the evaporation and condensation stages with the selected compressor.

The Table 6 reports the properties of a commercial PCM with a phase change temperature of 48°C.

Parameter	Value	Unit
Melting point	48	[°C]
Power density	57.5	[kWh/m^3]
Density (liquid)	820	[kg/m^3]
Density (solid)	900	[kg/m^3]
Thermal Conductivity (liquid)	0.15	[W/m°C]
Thermal Conductivity (solid)	0.25	[W/m°C]

Table 6: PCM material characteristics

1.6. Varna's demonstrator results

The Varna demonstrator aims to validate the feasibility and provide preliminary results regarding the integration of the various components described above, intending to recover waste heat from the data centre during the summer and reuse it in the district heating network during the winter.

The system layout selected for the Varna case study is shown previously in Figure 2. The following sections will present the parameters and connection strategies used to integrate the different components.

1.6.1. DC - PCM connection

In Figure 15, the connection between the DC cooling system and the PCM storage unit is illustrated. This subsystem is responsible for transferring the recovered heat to the seasonal storage system.

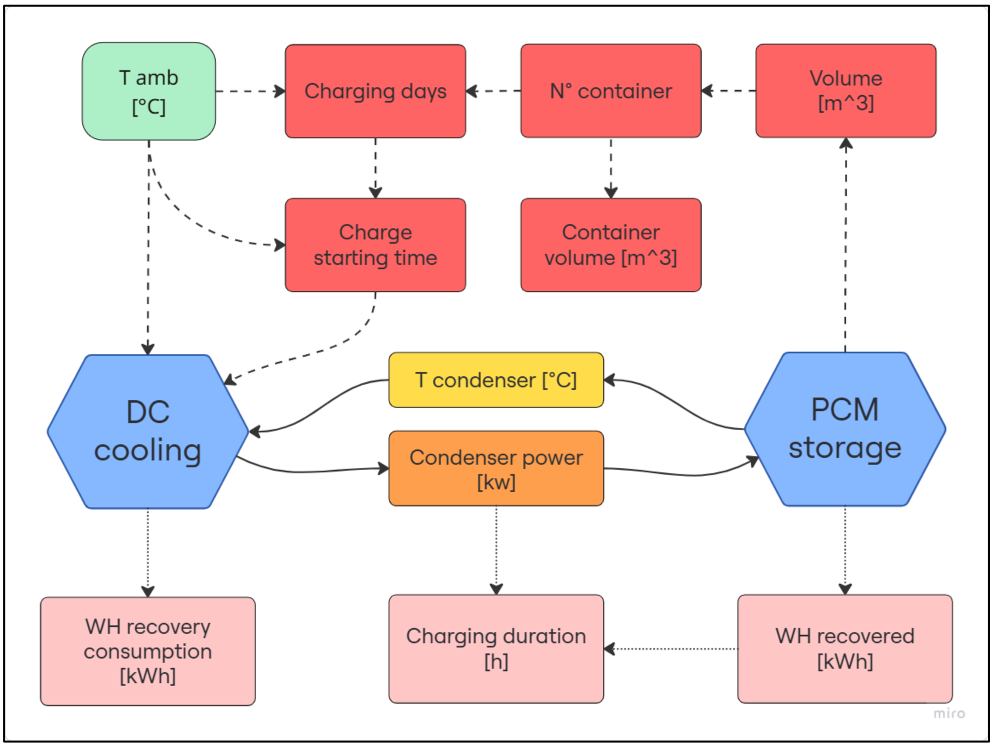

Figure 15: DC-PCM storage connection

The heat recovery from the DC to the PCM storage is carried out directly through the DC's cooling system, without the need for any additional device. This is possible because the charging temperature required by the PCM storage is 60°C, a value that can be directly achieved by the chiller used for cooling the DC. As shown in Figure 15, the condensation temperature is determined by the selected PCM material, while the thermal power available at the condenser depends on the data centre size and the cooling demand during the analysed hour.

The corresponding numerical values are shown in Figure 15 are reported in the Table 7.

Parameter	Value	Unit
Volume	13.16	[m^3]
Container volume	1.64	[m^3]
N° container	8	[-]
Charging days	8	[d]
Charge starting time	11:00 AM	[-]
T condenser	60	[°C]
Condenser Power	20.55	[kW]
Charging duration	5	[h]
WH recovery consumption	139.25	[kWh]
WH recovered	756.69	[kWh]

Table 7: DC-PCM storage connection results

The selection of the days for heat recovery follows a specific logic. The strategy is to charge one PCM storage module per day, meaning that the number of modules determines the number of recovery days. These days are selected based on ambient temperature during the summer period: the hottest days are chosen. This is because, on hotter days, chiller condensing temperature is naturally higher, this minimises the additional energy required to reach the PCM storage charging temperature and maximises the recovery efficiency. The Figure 16 shows the selected days for the PCM storage charging phase, based on Varna climatic data. The second column displays the average temperature during the charging hours for each of these days.

Index	Mean Temperature
2025-07-04 00:00:00	24.129
2025-07-11 00:00:00	24.267
2025-07-13 00:00:00	24.321
2025-07-18 00:00:00	24.2
2025-07-20 00:00:00	24.25
2025-07-22 00:00:00	24.479
2025-08-28 00:00:00	24.994
2025-08-29 00:00:00	24.127

Figure 16: PCM charge days

The charging phase duration depends on the amount of energy that can be stored in a single PCM module and the charging power. In this case, the charging duration is 5 hours, starting at 11:00 AM, to align with the warmest hours of the day, thereby minimising the additional energy consumption compared to standard chiller operation.

The number of containers is selected to ensure that each unit is easily transportable. The chosen commercial container size is 6 feet, corresponding to a volume of 5.8 m³. Considering the space required for auxiliary systems and the fact that the PCM material does not occupy the entire container volume, the maximum volume of PCM per module is set to 2 m³. This value is consistent with the specifications reported in D1.2 for the TCS system.

Figure 17 presents the main values related to the charging phase of the first two PCM modules.

Index	Temperature	DC_W_comp	PCM_W_charge	PCM_Q_charge	PCM_charge_consumption	Container	PCM_energy_accumulated	Total_energy_accumulated
2025-07-04 11:00:00	27.7	1.96	5.55	20.55	3.59	1	20.55	20.55
2025-07-04 12:00:00	28.2	2.02	5.55	20.55	3.53	1	41.1	41.1
2025-07-04 13:00:00	28.5	2.06	5.55	20.55	3.49	1	61.66	61.66
2025-07-04 14:00:00	28.9	2.11	5.55	20.55	3.45	1	82.21	82.21
2025-07-04 15:00:00	29.4	2.17	5.55	12.38	3.39	1	94.59	94.59
2025-07-11 11:00:00	28.8	2.09	5.55	20.55	3.46	2	20.55	115.14
2025-07-11 12:00:00	28.8	2.09	5.55	20.55	3.46	2	41.1	135.69
2025-07-11 13:00:00	30	2.24	5.55	20.55	3.31	2	61.66	156.24
2025-07-11 14:00:00	29.5	2.18	5.55	20.55	3.37	2	82.21	176.79
2025-07-11 15:00:00	29.5	2.18	5.55	12.38	3.37	2	94.59	189.17

Figure 17: PCM charging phase values

1.6.2. PCM - TCM storage connection

The Figure 18 illustrates the logic used to numerically connect the PCM storage system, responsible for heat transfer, with the TCM storage (TCS) system, which handles seasonal TES.

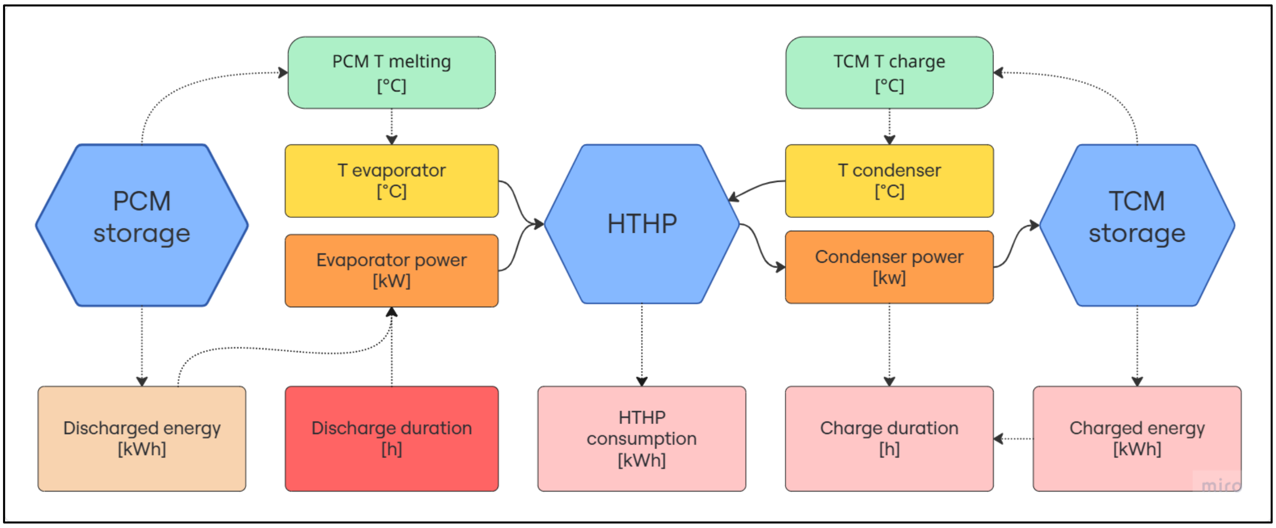

Figure 18: PCM-TCM storage connection

As shown in Figure 18, the component that enables heat transfer between the two storage systems is a HTHP. It is classified as high temperature because it must reach temperatures around 100°C in order to charge the TCM storage, and for "normal" and commercial heat pumps higher temperature is not more than 65°C

As illustrated in Figure 5, the heat pump requires as input the evaporator and condenser temperatures, as well as a power value between the evaporator and condenser. In this case, the evaporator power is provided as an input. This value is selected based on the desired duration of the PCM storage discharge phase, the power limitations imposed by the PCM storage, and the operating range of the available heat pump unit. The machine must operate within a defined power range, which must be respected.

The evaporator and condenser temperatures are selected based on the PCM discharge temperature ($T_{melting}$) and the charging temperature required by the TCM.

Once these values are defined, the model outputs include the electrical consumption of the heat pump, the amount of energy stored in the TCM, and the duration of the TCS charging phase.

In the analysed case, the values corresponding to the parameters and variables presented in Figure 18 are reported in Table 8.

Parameter	**Value**	**Unit**
PCM melting temperature	48	[°C]
T evaporator	60	[°C]
Evaporator power	15.13	[kW]
PCM Discharge duration	5	[h]
TCM T charge	100	[°C]
T condenser	112	[°C]
Condenser Power	25	[kW]
Charge duration	5	[h]
PCM discharged energy	605.35	[kWh]
HTHP consumption	394.65	[kWh]
TCM charged energy	1000	[kWh]

Table 8: PCM-TCM storage connection results

The TCS system itself is subdivided into eight 1.25 m^3 modules to enable continuous, controlled charging processes. This modular design allows each PCM storage unit to charge a corresponding TCS module, significantly optimizing the TCM charging phase. The complete charging characteristics for the TCS system are presented in Figure 19.

Ora	Container_PCM	Container_TCM	PCM_Q_discharge	TCM_W_charge	TCM_Q_charge	Energia_accumulata_TCM	Energia_scaricata_PCM	Energia_accumulata_per_TCM	Fase_carica
1	1	1	15.13	9.87	25	25	15.13	25	PCM1→TCM1
2	1	1	15.13	9.87	25	50	30.27	50	PCM1→TCM1
3	1	1	15.13	9.87	25	75	45.4	75	PCM1→TCM1
4	1	1	15.13	9.87	25	100	60.53	100	PCM1→TCM1
5	1	1	15.13	9.87	25	125	75.67	125	PCM1→TCM1
6	2	2	15.13	9.87	25	150	90.8	25	PCM2→TCM2
7	2	2	15.13	9.87	25	175	105.94	50	PCM2→TCM2
8	2	2	15.13	9.87	25	200	121.07	75	PCM2→TCM2
9	2	2	15.13	9.87	25	225	136.2	100	PCM2→TCM2
10	2	2	15.13	9.87	25	250	151.34	125	PCM2→TCM2

Figure 19: TCS charging characteristics

1.6.3. TCS - DHN connection

Figure 20 illustrates the numerical connections considered to link the TCM storage system with the DHN.

The logic adopted for simulating the discharge of energy from the TCM storage to the DHN is based on discharging one TCS container per day, continuously. As a result, the number of days during which the TCS provides heat to the DHN corresponds to the number of TCM containers available.

The discharge process is carried out using a HTHP, which must be condensed at a temperature higher than the DHN supply temperature, in order to effectively transfer heat to the network.

The selection of the discharge days is based on the DHN supply temperature. Specifically, the coldest days of the winter period, those with the lowest supply temperatures, are selected. This choice is made to optimize the heat pump's efficiency: when the supply temperature is lower, the heat pump can condense at a lower temperature, resulting in a higher COP and therefore reduced electricity consumption.

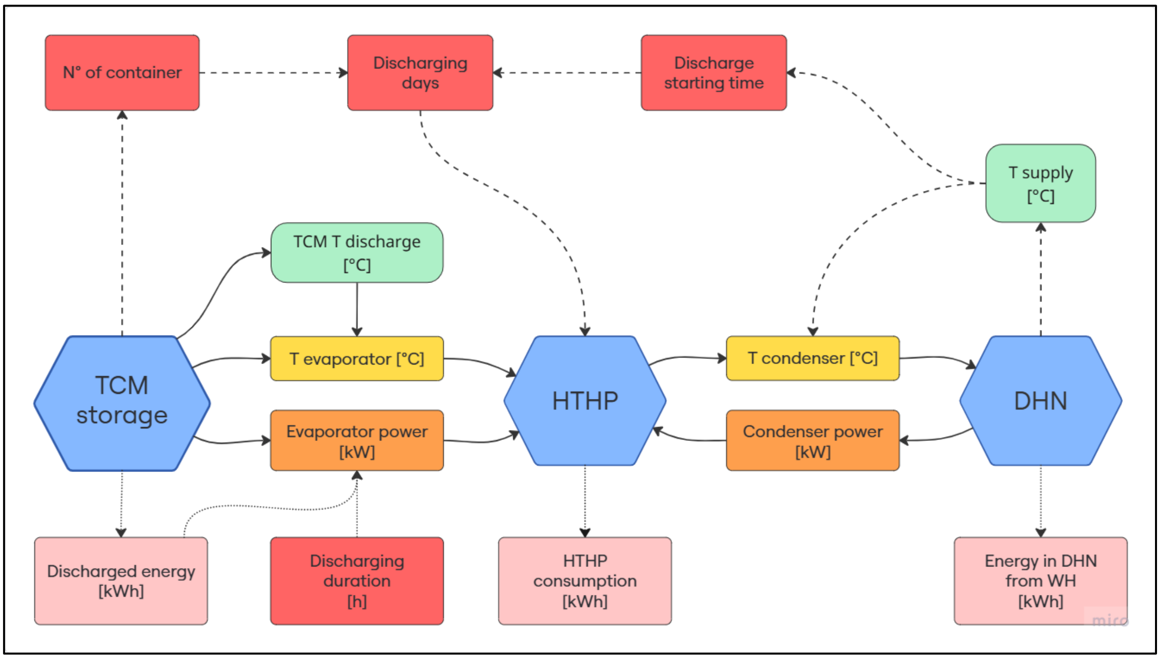

Figure 20: TCS-DHN connection

The evaporation temperature of the heat pump remains constant and is determined by the TCS discharge temperature, while the condenser temperature varies according to the DHN supply temperature at the analysed hour. As a result, the COP of the heat pump varies throughout its operating hours.

The evaporator power, and thus the TCS discharge power, is selected to achieve the desired discharge duration, while also complying with the operating limits of both the heat pump and the TCM storage system.

The detailed discharge characteristics of the TCM system, including temperature profiles and energy transfer rates, are presented in Figure 21.

Data_Ora	Container_TCM	T_supply	T_DHN_supply_HP	T_source	COP_HP	EER_HP	Q_out_TCM	W_HP	Q_in_DHN	En_out_TCM	En_in_DHN	En_out_TCM_tot	En_in_DHN_tot	Fase_scarico
2025-01-17 11:00:00	1	70.6	82.6	28	3.26	2.26	20	8.86	28.86	20	28.86	20	28.86	TCM1→DHN
2025-01-17 12:00:00	1	70.6	82.6	28	3.26	2.26	20	8.86	28.86	40	57.72	40	57.72	TCM1→DHN
2025-01-17 13:00:00	1	70.6	82.6	28	3.26	2.26	20	8.86	28.86	60	86.57	60	86.57	TCM1→DHN
2025-01-17 14:00:00	1	70.6	82.6	28	3.26	2.26	20	8.86	28.86	80	115.43	80	115.43	TCM1→DHN
2025-01-17 15:00:00	1	70.6	82.6	28	3.26	2.26	20	8.86	28.86	100	144.29	100	144.29	TCM1→DHN
2025-02-18 11:00:00	2	70.4	82.4	28	3.27	2.27	20	8.82	28.82	20	28.82	120	173.11	TCM2→DHN
2025-02-18 12:00:00	2	70.4	82.4	28	3.27	2.27	20	8.82	28.82	40	57.64	140	201.93	TCM2→DHN
2025-02-18 13:00:00	2	70.4	82.4	28	3.27	2.27	20	8.82	28.82	60	86.46	160	230.75	TCM2→DHN
2025-02-18 14:00:00	2	70.4	82.4	28	3.27	2.27	20	8.82	28.82	80	115.27	180	259.57	TCM2→DHN
2025-02-18 15:00:00	2	70.4	82.4	28	3.27	2.27	20	8.82	28.82	100	144.09	200	288.38	TCM2→DHN

Figure 21: TCS discharge characteristics

The model outputs include the electricity consumption of the HTHP, the energy discharged from the TCM, and the energy delivered to the DHN. This latter value represents the amount of energy that does not need to be supplied by the central heating plant, resulting in a net energy saving.

In the analysed case, the values corresponding to the parameters and variables presented in Figure 20 are reported in Table 9.

Parameter	**Value**	**Unit**
TCM T discharge	40	[°C]
T evaporator	28	[°C]
Evaporator power	20	[kW]
TCM Discharge duration	5	[h]
N° of container	8	[-]
Discharging days	8	[d]
Discharging starting time	11:00 AM	[-]
T supply	70.3 – 70.8	[°C]
T condenser	82.3 – 82.8	[°C]
Condenser Power	28.82 – 28.9	[kW]
TCM discharged energy	800	[kWh]

HTHP consumption	354.13	[kWh]
Energy in DHN from WH	1154.1	[kWh]

Table 9: TCS-DHN connection results

1.6.4. System results

The results of the overall system are summarised in Table 10.

Parameter	**Value**	**Unit**	**Notes**
Energy in DHN	1154	[kWh]	-
Total consumption	888	[kWh]	-
Energy saving	115.41	[kWh/m^3]	Energy in DHN / TCM volume
System efficiency	1.3	[-]	Energy in DHN / Total consumption

Table 10: System performances

The Figure 22 graphically presents the total electrical energy consumed in comparison to the thermal energy supplied to the district heating network.

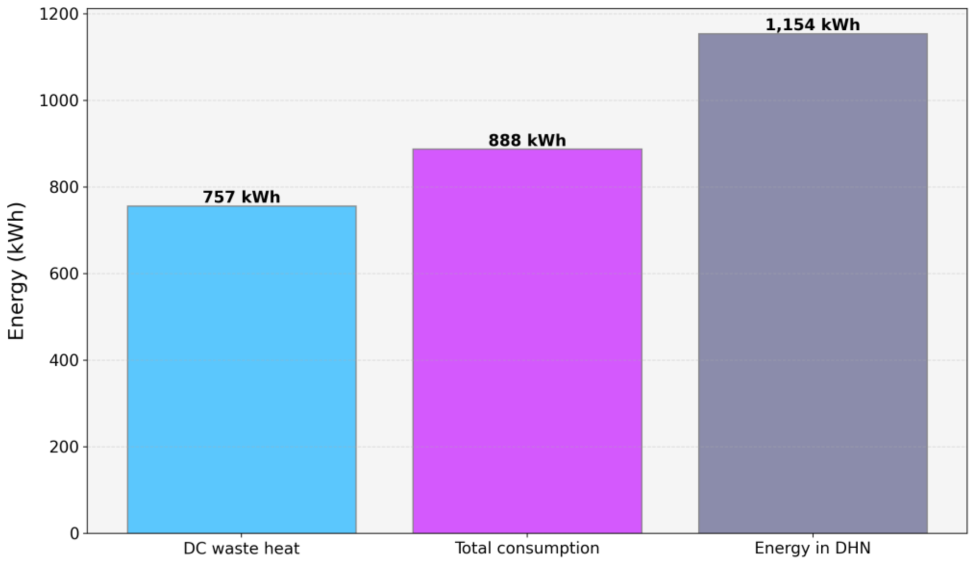

Figure 22: DC waste heat recovered vs. Total consumption vs. Energy in DHN

The Figure 23 shows the composition of energy consumption distributed among PCM charging, TCM charging, and TCM discharging.

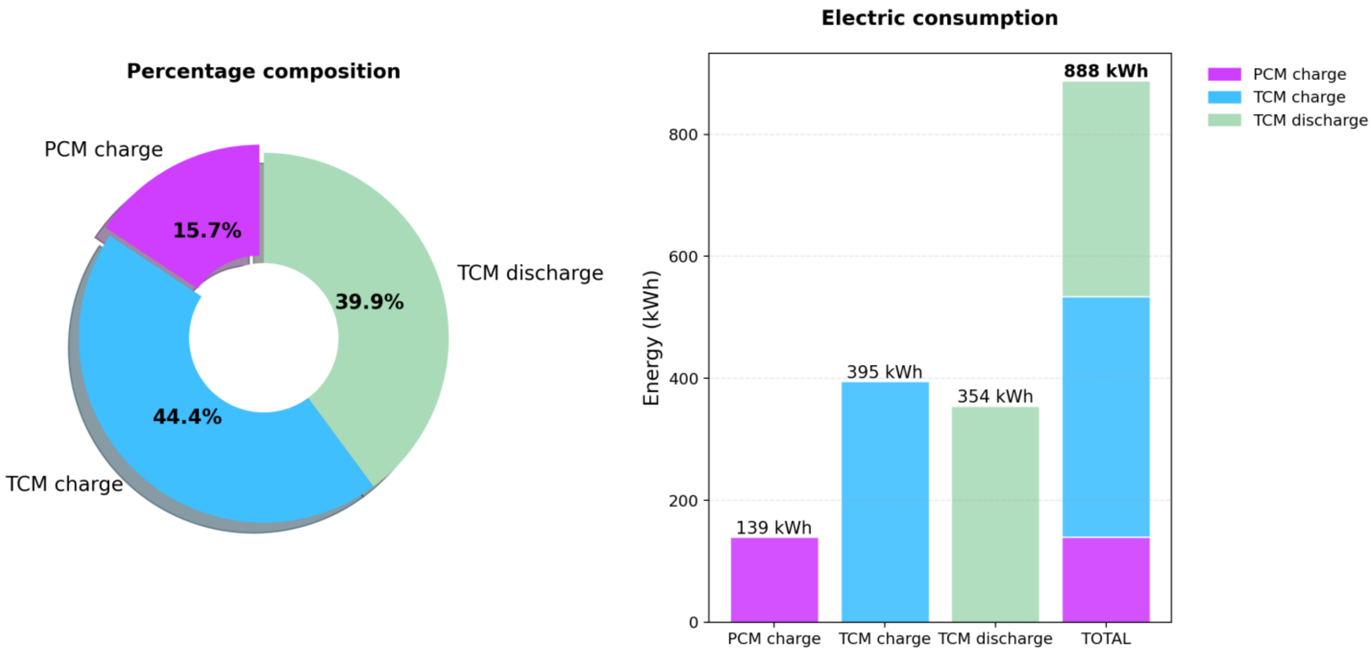

Figure 23: Composition of electric consumption

2. Replicability of THUNDER concept

This section of the deliverable introduces the concept of replicability of the THUNDER solution.

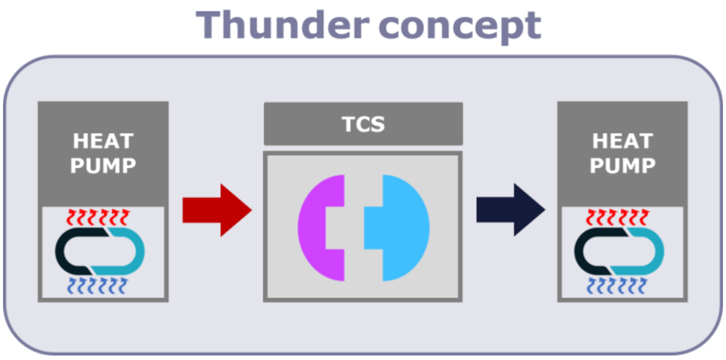

Figure 24: THUNDER concept

Figure 24 provides a schematic representation of the THUNDER concept, which is based on the seasonal storage of excess heat through TCM storage (TCS) system. The charging phase of the TCM is carried out using an innovative HTHP. During the discharging phase, a second heat pump is employed to upgrade the energy released by the TCM, originally at the material's characteristic discharge temperature, to the temperature level required by the end-user.

This configuration enables an efficient and flexible integration of waste heat recovery into heating networks, supporting the scalability and adaptability of the solution in different climatic and operational contexts.

Building on the central role of the THUNDER concept, a set of potential scenarios is presented to assess its performance under varying boundary conditions. The objective is to demonstrate the replicability of the proposed solution across different case study typologies, extending beyond the specific context of the Varna demonstrator.

For all scenarios, the general system layout will be presented, along with the connections implemented in the code to enable communication between the various components described in 1.4.

2.1. Replicability scenarios

2.1.1. DC-DHN direct connection through TCM seasonal storage

The first scenario considered, which is shown in Figure 25, involves the presence of a data centre located in proximity to a district heating network, enabling a direct connection between the two systems. The operational principle relies on storing waste heat from the DC in the TCM storage during the summer period, when cooling is provided by chillers, and subsequently discharging it into the DHN during the winter season, when the thermal demand from connected users is significantly higher.

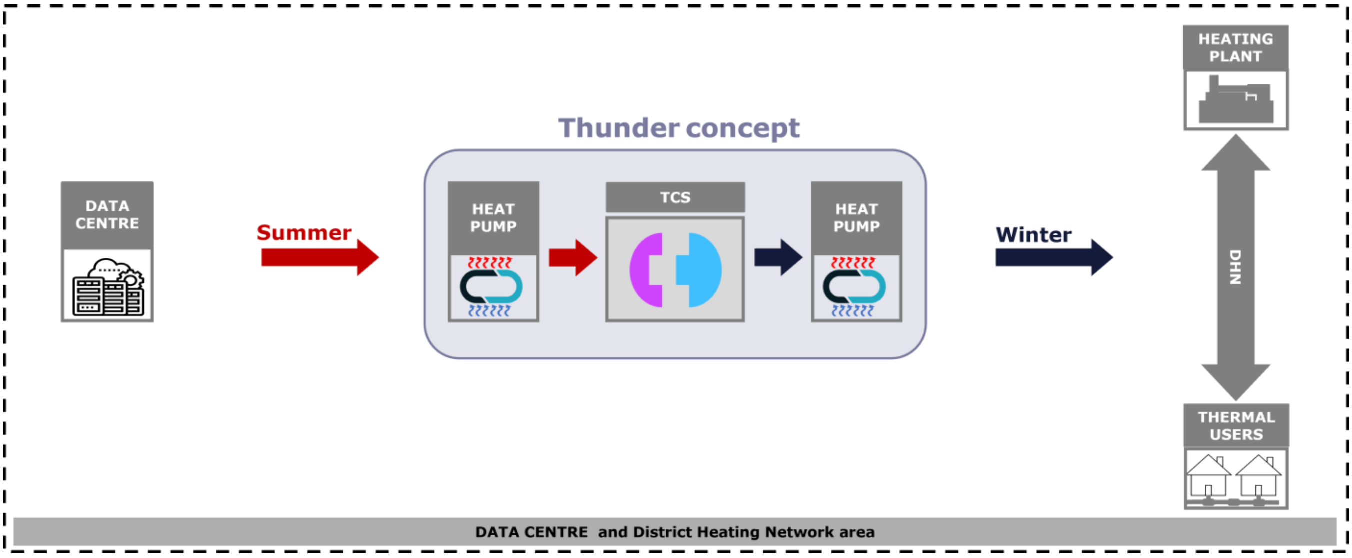

Figure 25: DC-DHN direct connection through TCM seasonal storage (TCS)

In this scenario, there are two main connections between the system components. The first concerns the link between the data centre and the seasonal TCM storage (TCS), as shown in Figure 26. The second refers to the connection between the TCM storage and the DHN, where the recovered waste heat is discharged, as illustrated in Figure 27.

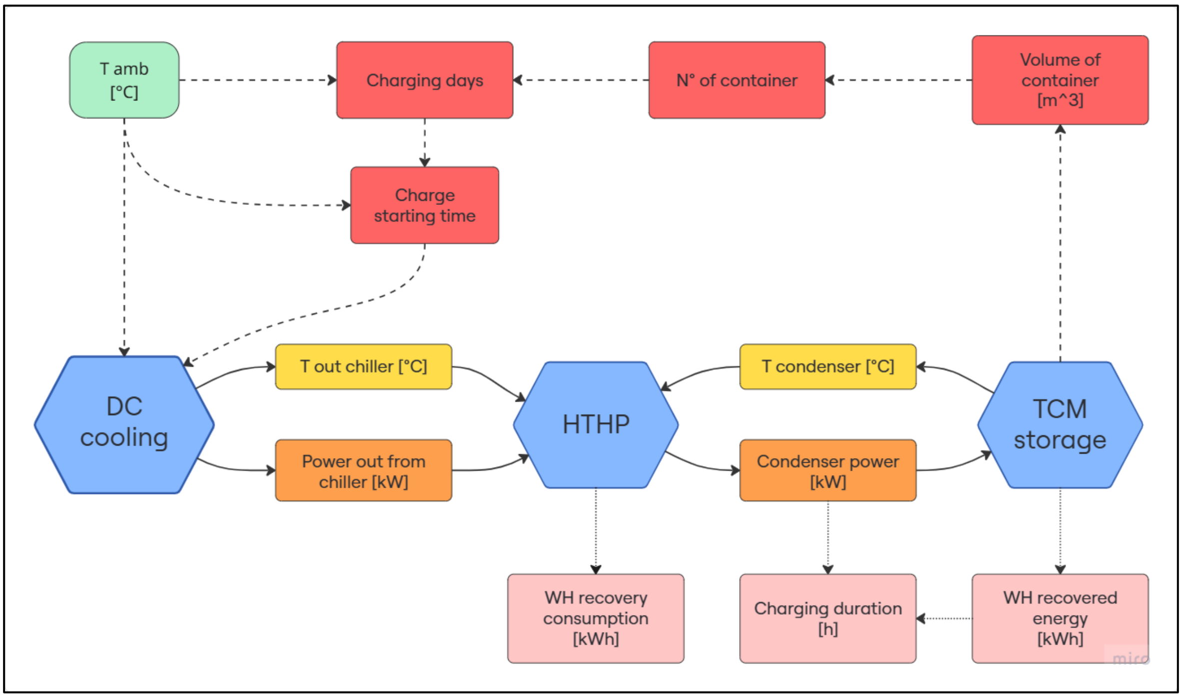

Figure 26: DC-TCM storage connection

In this scenario, a HTHP is required to charge the TCM storage until research leads to the development of a material with suitable properties and a sufficiently low charging temperature that can be reached directly by the chiller. Therefore, it is necessary to couple the HTHP with the DC's cooling system.

In this configuration, the evaporator temperature and evaporator power of the HTHP are directly linked to the chiller's condensation temperature and the thermal power it releases. Another input to the heat pump is the condenser temperature, which corresponds to the charging temperature of the selected TCM material. Once these parameters are defined, the heat pump is fully characterised, and the condenser power can be calculated accordingly.

After determining this value, it is necessary to verify whether the TCM storage system can receive the calculated power. If not, part of the heat must be dissipated, or a lower amount of heat should be recovered from the data centre.

To determine when to perform the heat upgrade, it is assumed that once the container volume and number of units are defined, one container is charged per day. This assumption provides the number of days during which heat recovery is performed. The selection of these days is based on ambient temperature, prioritising the warmest days, to minimise energy consumption, as previously explained in 1.6.

Once all the necessary parameters are selected, the model can compute the HTHP electricity consumption, the amount of energy stored in the TCM, and the duration of the charging phase.

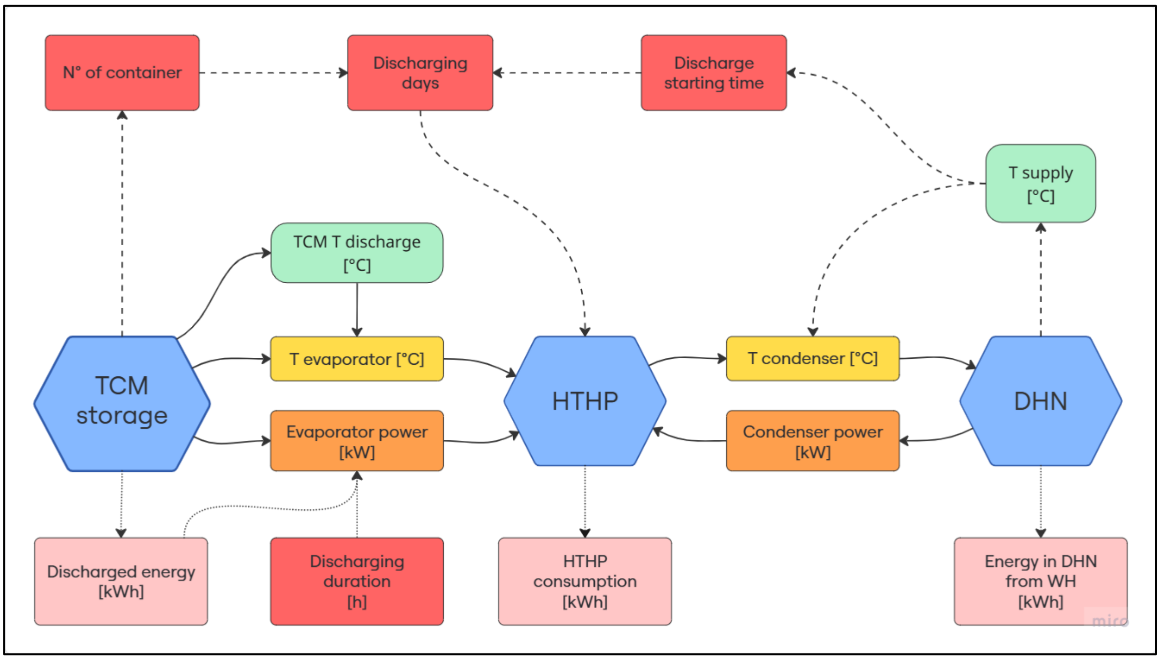

Figure 27: TCM storage-DHN connection

Concerning the connection between the TCM storage and the DHN, the considerations are entirely analogous to those described in the demonstrator case (see 1.6.3)

2.1.2. DC waste heat integration in DHN through PCM “Heat on Wheels” and TCM seasonal storage

In cases where heat transport is required due to the distance between the data centre and the district heating network, PCM storage technology is introduced. Two sub-cases can be identified.

The first, analogous to the demonstrator scenario, involves coupling the PCM storage with the data centre to recover waste heat and transport it to the TCM storage, which in this case is located near the DHN.

Alternatively, the TCM storage can be placed near the DC, allowing it to recover waste heat directly (as shown in Figure 26). In this configuration, the PCM storage is used during the winter to discharge the TCS, enabling the transport of heat to the end-user, which in this case is represented by a DHN.

2.1.2.1. PCM storage connected with DC

This configuration (Figure 28) exactly mirrors the one presented in 1.6

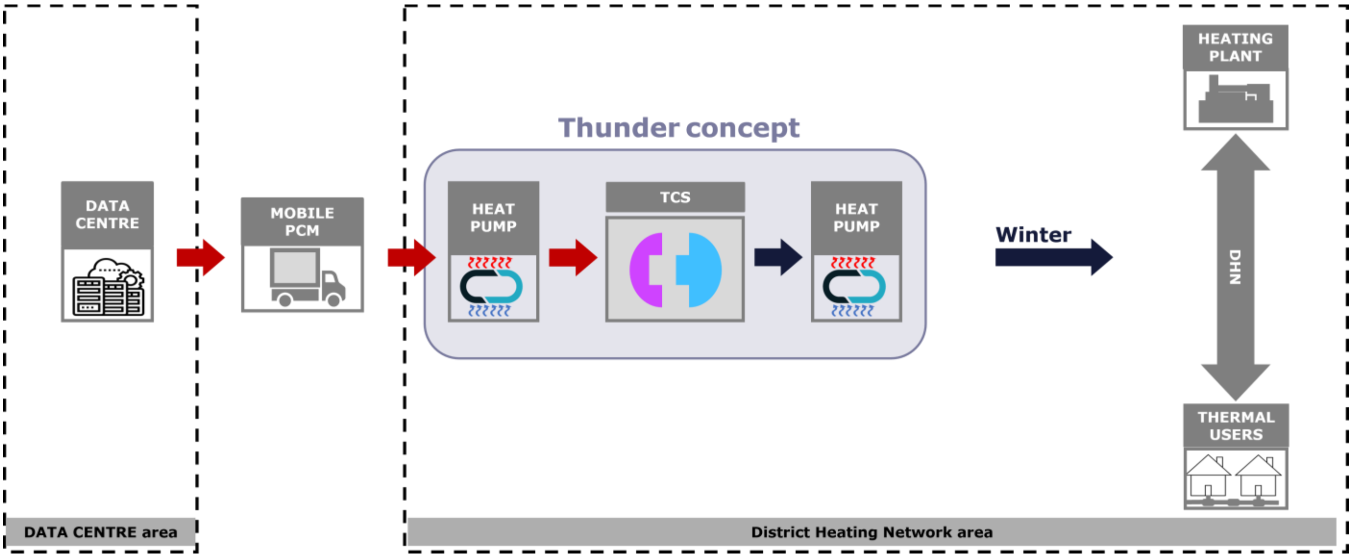

Figure 28: DC waste heat integration in DHN through PCM heat on wheels and TCM seasonal storage

The connections between the various components in this case are as follows:

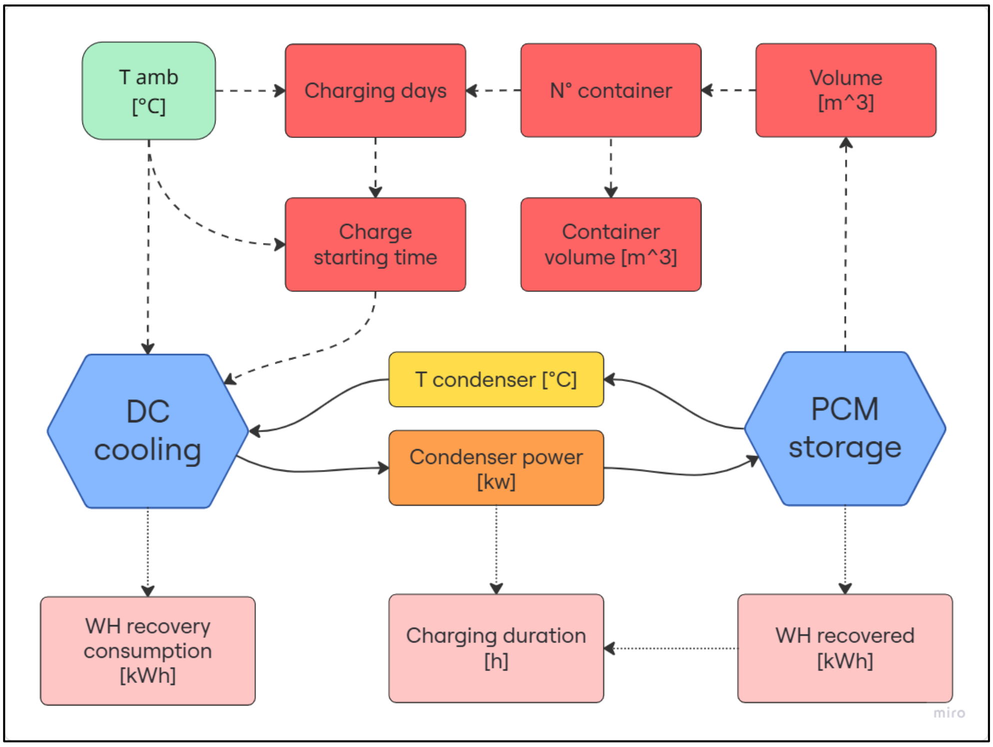

Figure 29: DC-PCM storage connection

The connection between DC and PCM is shown in Figure 29 and described in 1.6.1

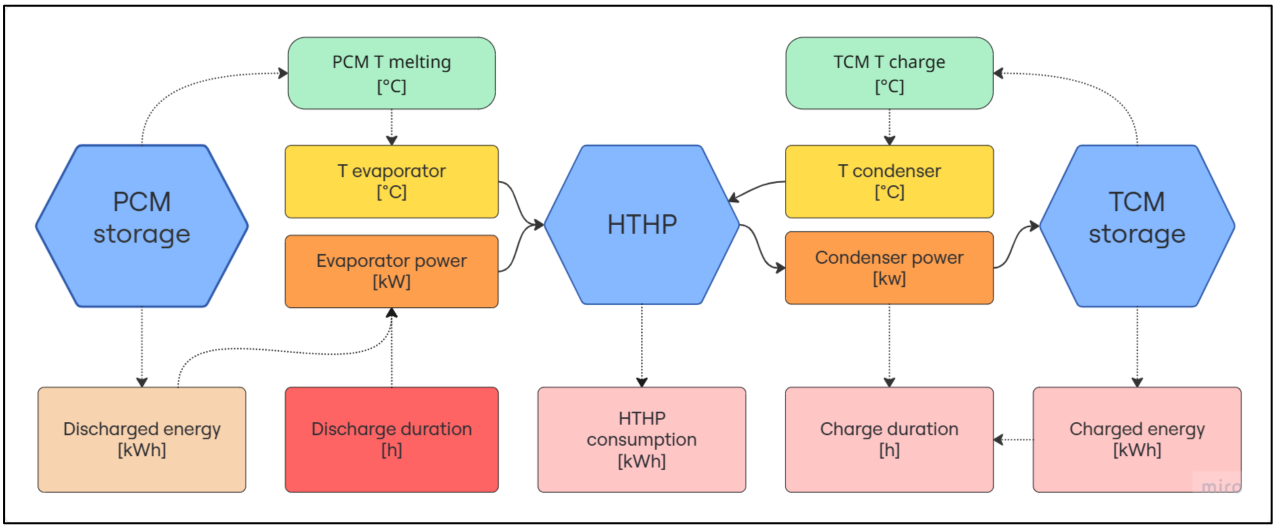

Figure 30: PCM storage-TCM storage connection

The connection between PCM and TCM storages is shown in Figure 30 and described in 1.6.2

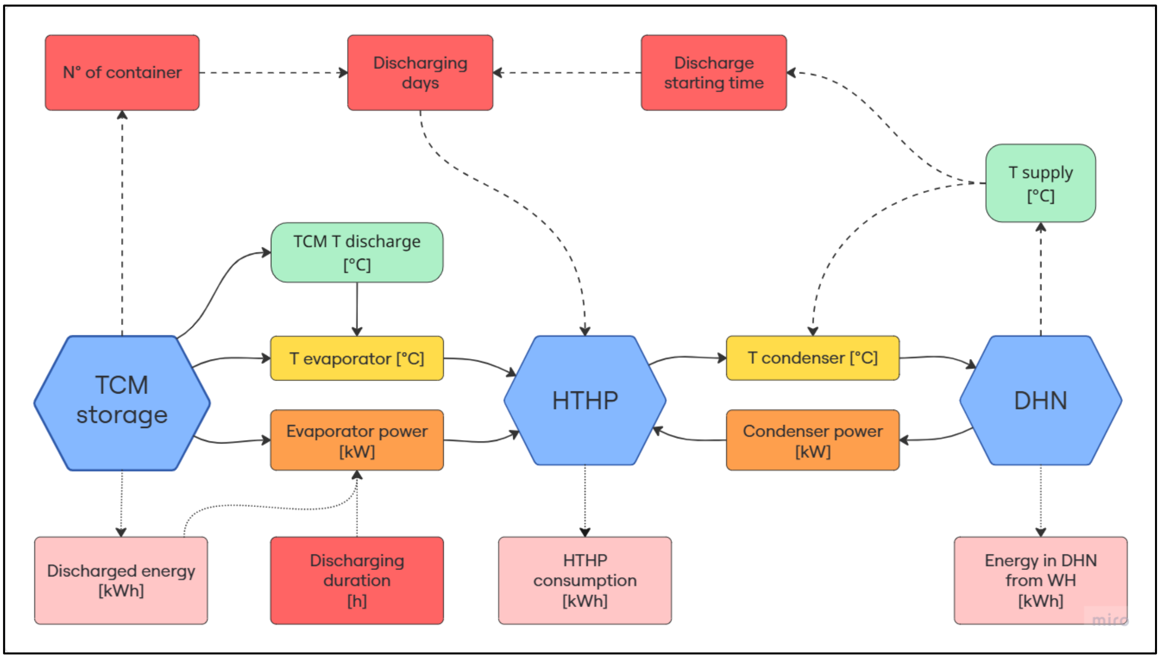

Figure 31: TCM storage-DHN connection

The connection between TCM storage and DHN is shown in Figure 31 and described in 1.6.3

2.1.2.2. PCM connected with DHN

This scenario, shown in Figure 32, arises when the DC can host the seasonal storage. In this case, the waste heat generated by the data centre is directly stored in the TCS during the summer. During the winter, the stored heat is transported to the end-user, represented in this case by the DHN using PCM-based "Heat on Wheels" technology.

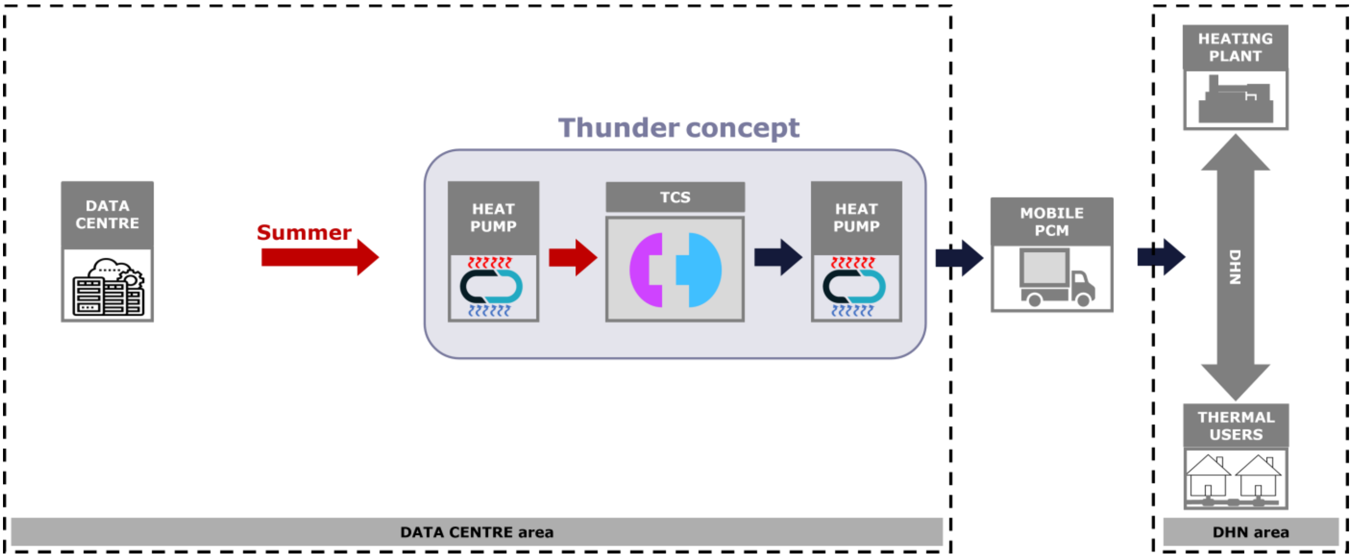

Figure 32: DC waste heat integration in DHN through TCM seasonal storage and PCM "Heat on Wheels"

The first connection, shown in Figure 33, in this case links the DC with the TCM storage system to enable waste heat recovery. For a detailed description, please refer to 2.1.1.

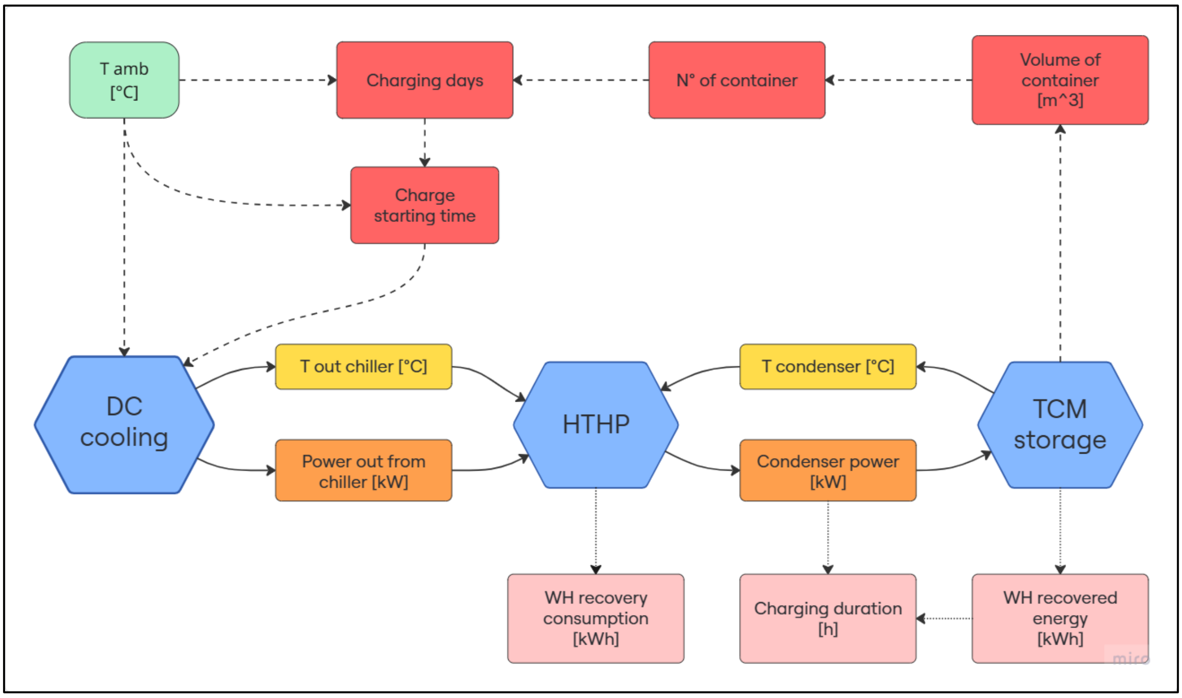

Figure 33: DC-TCM storage connection

The second connection (Figure 34) links the TCM storage system with the PCM storage ("Heat on Wheels"). This connection is activated during the winter period, allowing the transfer of heat accumulated and stored in the TCS during the summer to the mobile PCM unit, so that it can be transported to the end-user requiring thermal energy.

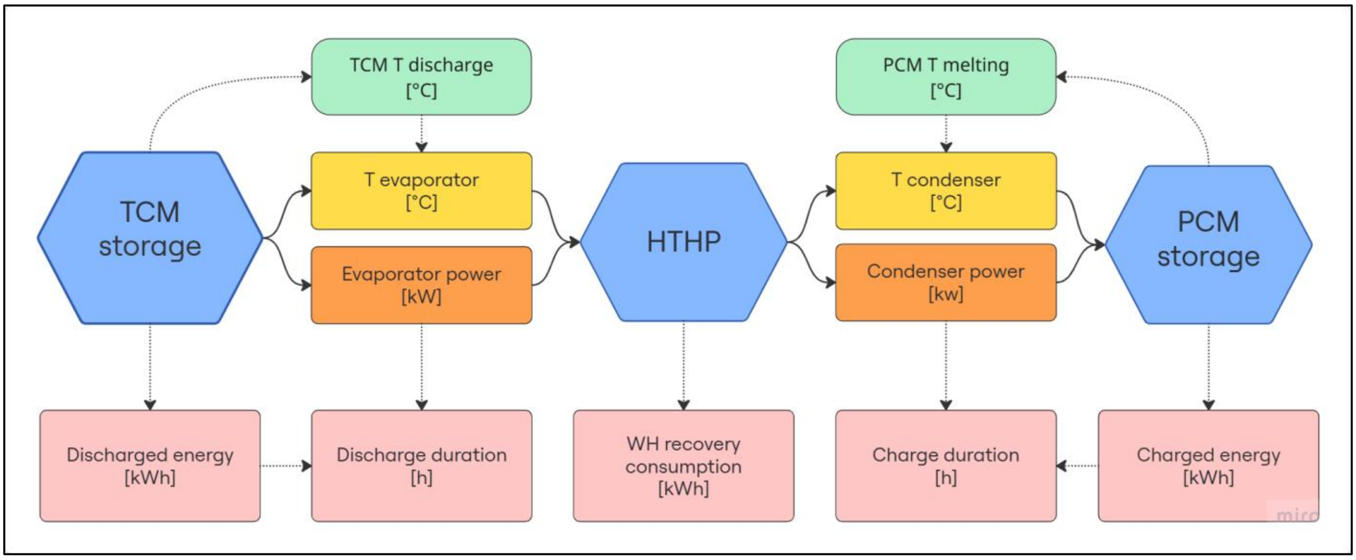

Figure 34: TCM storage - PCM storage connection

In this case, a PCM material with a phase change temperature higher than the temperature required by the end-user has been selected. This allows the discharge to the user to occur without additional energy consumption. Since the end-user is a district heating network with a supply temperature above 80°C, HTHP is required to transfer heat from the TCM storage to the PCM storage.

However, if the end-user operates at a lower temperature, it is possible to envision a configuration where the heat pump is not needed. Specifically, if the condition $T_{user} < T_{PCM} < T_{TCM}$ is met, the discharge from the TCM storage to the PCM storage and from the PCM storage to the user could occur without any additional energy input.

Nevertheless, this assumption is considered too restrictive for broader applicability across different scenarios and has therefore not been adopted in the current analysis.

Once the TCM and PCM materials are selected, the operating temperatures of the HTHP are also defined. On the evaporator side, the temperature corresponds to the TCM discharge temperature, while on the condenser side, it matches the melting temperature of the PCM.

After setting these thermal levels, the next step is to select the size of the heat pump, which must comply with the acceptable power ranges for both TCM discharge and PCM charging. One of the two power values is selected, and the other is then calculated accordingly.

At this point, the model can compute the output values, which include the energy discharged from the TCM, the electricity consumption of the HTHP, the amount of energy stored in the PCM, and the duration of the operation.

The final connection in the following scenario is between the PCM system and the end-user (Figure 35), which in this case is the district heating network. This case illustrates a situation where the PCM storage system delivers heat at a higher thermal level than that required by the user. As a result, there is no need for a heat pump between the two components; only a heat exchanger is required to enable heat transfer between the two flows. The input values include the thermal power transferred, which is used to calculate the duration of the PCM discharge phase. Another output value is the amount of energy supplied to the user, which corresponds to the resulting energy savings. Logical parameters include the days and time slots during which the discharge is carried out. This choice is based on the number of available PCM containers and the supply temperature of the district heating network.

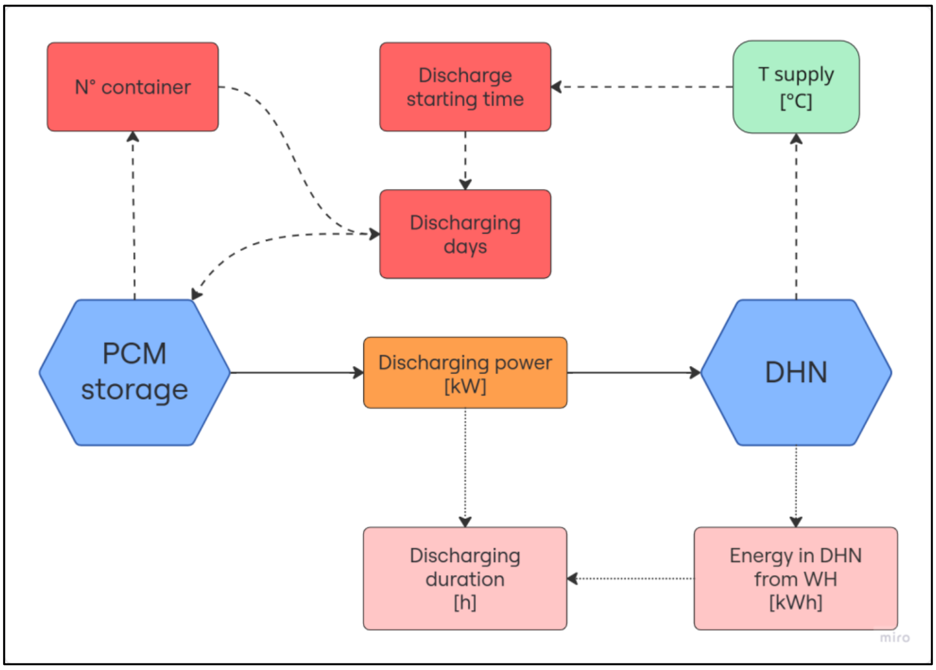

Figure 35: PCM storage-DHN connection

2.1.3. DC waste heat integration in DHN through TCM seasonal storage and two PCM heat on wheels

Another scenario occurs when the seasonal storage cannot be located near either the DC or the DHN. In this case, the use of two-PCMs with different phase change temperatures is proposed. The first PCM is selected with a temperature suitable for direct use by the data centre's chiller, while the second PCM has a phase change temperature higher than the DHN supply temperature, enabling direct heat discharge from the PCM to the network.

The operational scheme involves storing the waste heat from the DC in the first PCM during the summer, then transporting this PCM storage at the location of the seasonal TCM storage. The heat is then transferred from the first PCM to the TCM storage, which minimizes thermal losses to the environment. During winter, the heat stored in the TCM is discharged into the second PCM at a temperature higher than the DHN supply temperature. This second PCM storage is then transported close to the DHN, where the heat is directly delivered to the network. This scenario is illustrated in the Figure 36.

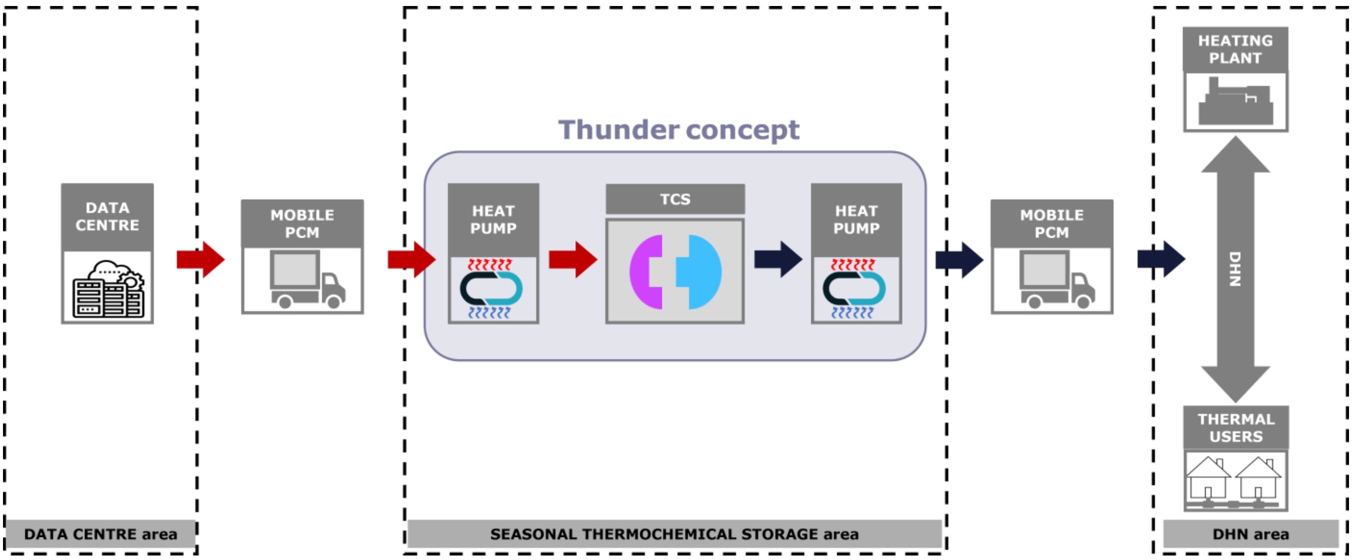

Figure 36: DC waste heat integration in DHN through TCM seasonal storage and two PCM heat on wheels

The connections present in this scenario have already been introduced in the previous scenarios. In particular, the one between DC and PCM storage is shown in Figure 37 and was described in 1.6.1.

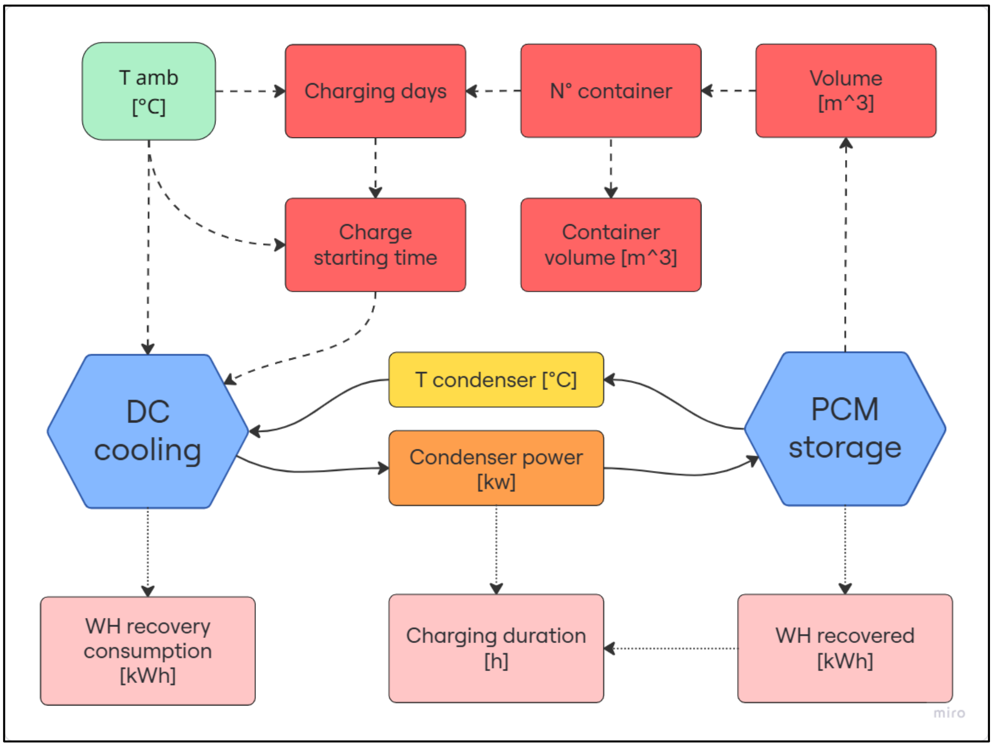

Figure 37: DC-PCM connection

The connection between PCM and TCM storages is shown in Figure 38 and described in 1.6.2

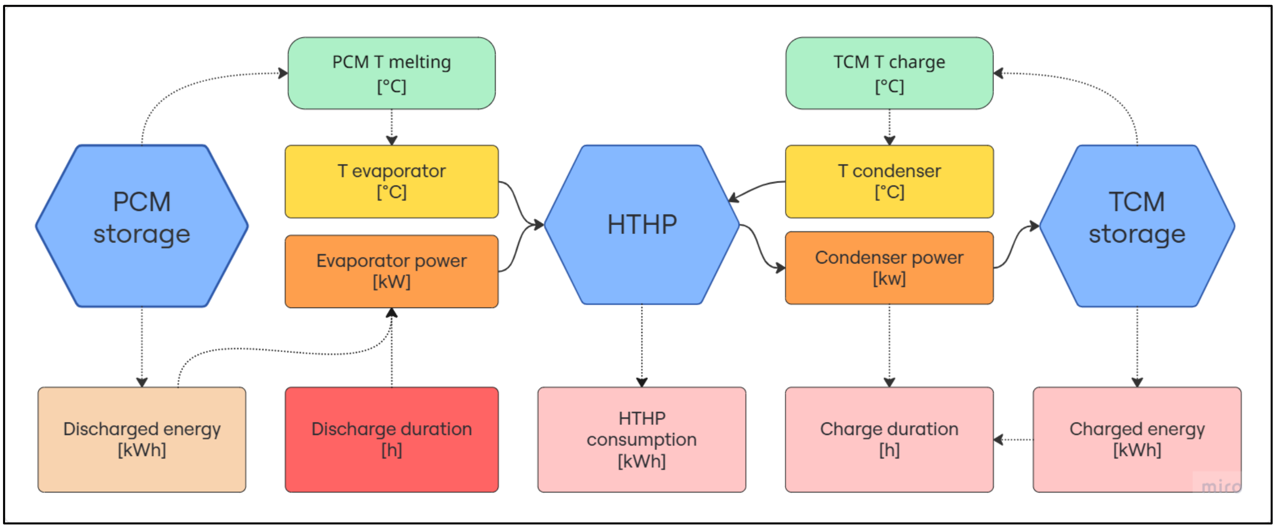

Figure 38: PCM-TCM storages connection

The connection between TCM and PCM storages is shown in Figure 39 and described in 2.1.2.2

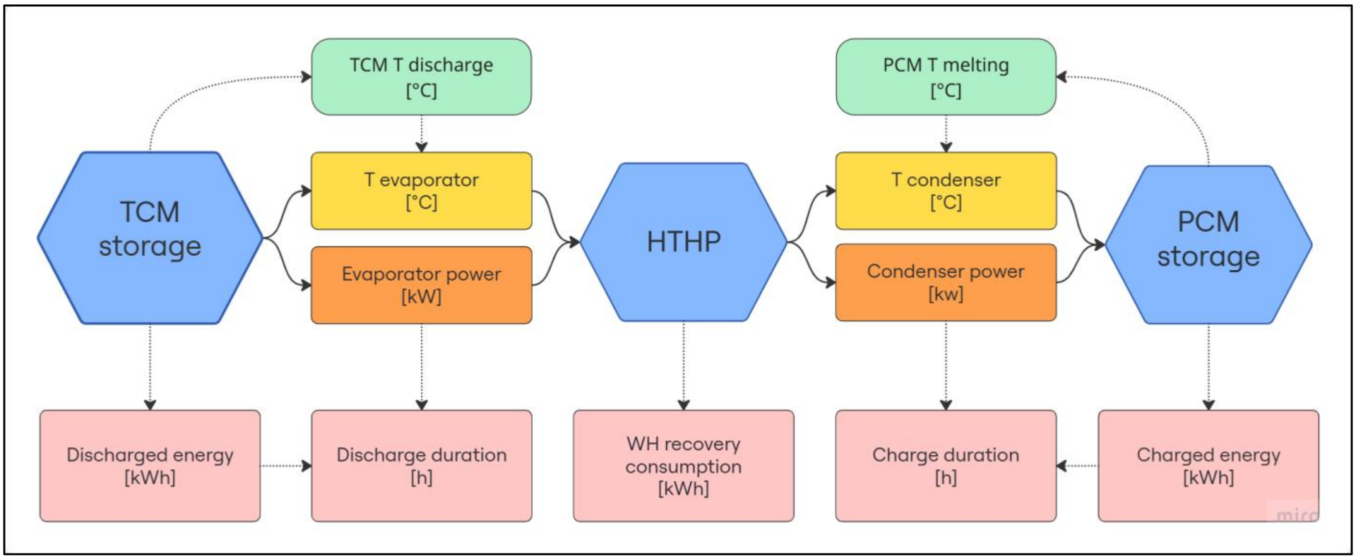

Figure 39: TCM-PCM storages connection

And the connection between PCM storage and DHN is shown in Figure 40 and described in 2.1.2.2.

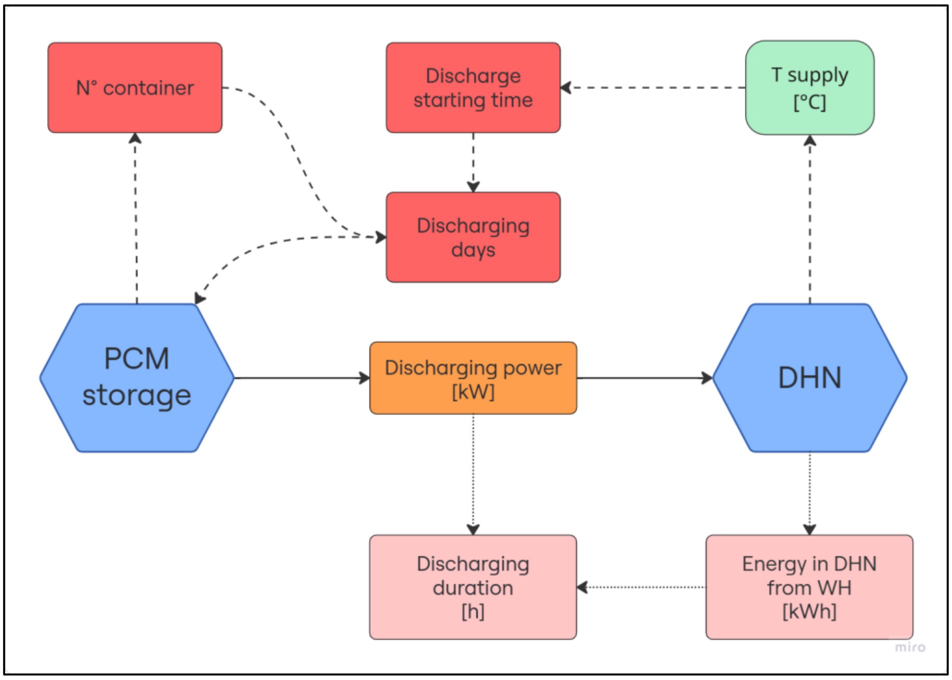

Figure 40: PCM storage -DHN connection

2.1.4. Waste heat logics

For each of these scenarios, two different simulation approaches are proposed, reflecting distinct strategies for the accumulation and reuse of waste heat generated by the data centre.

The first approach consists of defining the capacity of the TCM storage as a percentage of the waste heat available from the DC. In the analysed case, a recovery rate of 5% of the heat discharged from the chiller condenser was selected. This method sets the seasonal storage capacity a priori, allowing the storage volume to be easily calculated once the energy density of the chosen material is known.

This approach mirrors the conditions of the Varna demonstrator, where the TCM volume is treated as a boundary condition. Based on this fixed volume, all control strategies, such as module subdivision, selection of charging days, and other parameters described in the section 1.6, are defined accordingly. The heat recovery percentage may vary depending on the limitations and specifics of the case under study. Since no specific case study is considered at this stage, the 5% value was chosen as a reference.

The second control strategy aims to recover the entire amount of waste heat produced by the DC during the summer or within a defined period of the summer season. In this case, the required storage volume is not known in advance but is an output of the simulation and needs to be evaluated considering the modular concept requested by the heat on wheels solution.

These two distinct control strategies were chosen to represent two different perspectives on the problem. The first assumes the availability of a fixed storage volume or energy capacity, aiming to recover the maximum possible amount of energy within the given spatial constraints. The second focuses on recovering the entire possible amount of waste heat without considering limitations related to storage volume or space.

2.2. Replicability results

This paragraph presents the results of the simulations related to the scenarios described in the previous chapter.

The numerical simulation tool developed in Task 1.1.2 enables the configuration of a vast range of application scenarios. However, exploring the full extent of possible combinations or conducting comprehensive parametric analyses seems not feasible within the scope of the present document. Instead, a selection of 'reference' scenarios is presented to demonstrate the tool's flexibility and to provide insights into energy performance, associated quantities, and dimensional requirements. These results serve as a basis for assessing the scalability and replicability of the model proposed in the project.

Four scenarios will be evaluated, representing the extent of the admissible range in terms of "distance" in connection and of energy flow management. The first scenario is related to a "short distance", a direct connection between the DC and the DHN is established via TCM storage; TCS, as illustrated in Figure 25 will be presented considering two energy control strategies: a case where 5% of the waste heat from the data centre is recovered, and the case where the waste heat generated between June and September is entirely recovered.

The other two scenarios are related to "large distance" to be covered by the heat on wheels solution from DC and DHN, where the TCM storage; TCS is located remotely from both the DC and the DHN. In this case, two different PCM storages are used to transport heat from the DC to the TCS and from the TCS to the DHN, respectively. Results for this scenario, shown in Figure 36 will also be presented for the two energy control strategies: recovery of 5% of the waste heat and recovery of all the heat produced from June to September.

The Table 11 provides a summary of the simulated scenarios along with their respective characteristics. For simplicity, from this point onward, the following scenarios will be referred to by the names assigned below.

	Direct connection	**Two PCM storages**	**5% of waste heat recovered**	**Waste heat recovery June-September**
Scenario 1	✅		✅	
Scenario 2	✅			✅
Scenario 3		✅	✅	
Scenario 4		✅		✅

Table 11: Replicability scenarios whose results are presented

For the replicability analysis, a DC with characteristics similar to those of the Varna case study was selected, but with a higher power capacity (100 kW) and a cooling system based on conventional free cooling techniques (either direct or indirect). The results achievable with this configuration are proportionally scalable in terms of energy performance and overall system efficiency as the power level varies. Different IT technologies and functions within the data centre, which may generate usage profiles and consequently waste heat generation patterns, substantially different from those considered in this context, have not been detailed here but can be easily incorporated and addressed by the simulation tool. Unlike the Varna demonstrator case, in this simulation, a cooling system employing free cooling is used when the outdoor temperature falls below 15°C. The chiller operates only during periods when the ambient temperature exceeds this threshold, meaning that free cooling is not available during those times. Consequently, waste heat is considered only from the chiller condenser when the chiller is in operation. In a climate like Varna's, the cooling system can operate using free cooling for 5,237 hours, which corresponds to 59.80% of the total annual hours. The modular approach remains under consideration, employing standard containers whose dimensions and quantities are determined according to the required TES and the daily charging and discharging operations of the TCM storage.

The data centre's energy consumption when operating independently is shown in Figure 41.

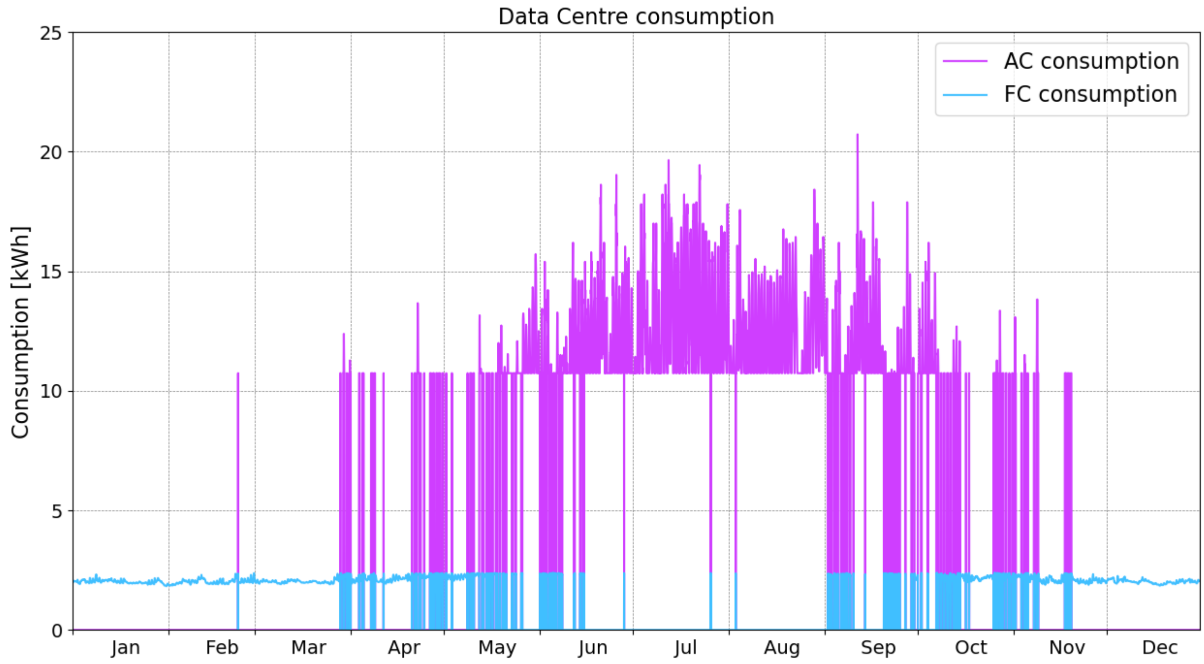

Figure 41: 100kW DC consumption with FC

The Table 12 presents data related to the data centre when it is not connected to a heat recovery system.

Parameter	**Value**	**Unit**
DC Nominal power	100	[kW]
DC consumption	49.77	[MWh]
DC total waste heat	906.05	[MWh]
DC active cooling of waste heat	382.35	[MWh]

Table 12: DC results

The next paragraphs introduce general info and boundary conditions about the considered scenarios, introducing the characteristics and performance parameters of the devices that have to be considered in the suitable energy chain as described in the previous chapters 1.6 and 1.7. Results will be presented in comparative tables, in a dedicated chapter 1.9.

2.2.1. Scenario 1

Scenario 1 refers to the case where the data centre and the district heating network are located close to each other and can be directly connected through TCM storage. In this scenario, the recovery of 5% of the waste heat exiting the chiller condenser is considered. When heat is not recovered, it is released into the environment through a dry cooler; when heat recovery is performed, a heat pump is used to accumulate the heat in the TCS. Thermodynamic assumptions on thermochemical regeneration process temperature and connections with charging addresses on a condensing temperature level of the HTHP near 110°C. The evaporator temperature at DC Cooling (set at 15°C) impose then a high temperature lift and it suggest to introduce an intermediate temperature level, as the quadratic mean between those two temperature values (that's is 60°C) where put the condensing process of the data centre cooling and the evaporation process of the high temperature heat pump. This process can be easily performed by hydraulic circuits with a suitable inertial tank.

The DC's waste heat amounts to 906.05 MWh per year, considering both free cooling and air conditioning operational modes. The heat from the air conditioning mode is 382.35 MWh. The TCS capacity is thus selected by calculating 5% of the waste heat during the air conditioning mode, resulting in 19.1 MWh. Considering the energy density of the material, this corresponds to a total volume of 191 m³.

To enable continuous charging of the TCS throughout the day, the system has been divided into separate containers, allowing each container to be charged independently. This configuration prevents the risk of unintentional discharge of the storage system due to contact with external air during periods when charging is not possible (i.e., during hours when the data centre operates in free cooling mode).

2.2.2. Scenario 2

Scenario 2 illustrates the configuration of a direct connection as in *Scenario 1*, but in this case, the analysis focuses on recovering all the waste heat during the period from June to September.

In this case, to enable heat recovery during all air conditioning hours between June and September, it is assumed that the TCS allows for non-continuous charging, meaning that pauses during the charging phase are possible. This assumption implies that this scenario can only be considered if discontinuous charging operation of the TCS can be ensured.

The considerations regarding the operating temperatures of the heat pumps, the DC's energy consumption when heat recovery is not performed, and the waste heat generated by the DC remain the same as in Scenario 1.

The energy that can be stored in the TCS amounts to 500.59 MWh, corresponding to a total volume of 5006 m³. The number of containers used to subdivide this volume is determined by considering two factors: first, the spatial limitation to fit within a 20-foot container (this sizing allows the use of commercially available containers, which are easy to source and do not require special transport arrangements or present other logistical issues that would arise with larger dimensions), and second, the need to fully charge all containers during the analysed period.

Taking these aspects into account, the chosen number of containers is 381, resulting in a volume of 13.14 m³ per container. Given the power levels involved, the duration of the charging phase is 7 hours.

Regarding the discharge phase in this scenario, it is assumed to occur continuously during the period from November to February. During this time, the various TCS containers are discharged consecutively and continuously to cover the maximum number of hours within the analysed period, ensuring that all containers are fully discharged.

Based on these assumptions, the TCS discharge phase lasts 2,667 hours out of the 2,880 hours between November 1st and February 28th. This allows maintaining a constant power output of 209.66 kW to the district heating network (DHN) for 92.6% of the selected period.

2.2.3. Scenario 3

Scenario 3 represents the case in which the data centre, the seasonal TC, and the DHN are all located at a distance from each other, necessitating the use of a HoW storage system to enable transport between components. Two different PCMs are employed because operation is required at different thermal levels.

The first PCM, which recovers heat from the data centre and transfers it to the TCS, will operate in the same manner as in Varna demonstrator as described in the paragraph 1.6.1. The second PCM, which extracts the stored heat from the TCS and transports it near the end user, in this case, the Varna district heating network, has a melting temperature higher than the DHN supply temperature. This allows direct discharge of the PCM without the need for an additional heat pump. The characteristics of the second PCM are reported in Table 13.

Parameter	Value	Unit
Melting point	86	[°C]
Power density	50.82	[kWh/m^3]
Density (liquid)	800	[kg/m^3]
Density (solid)	870	[kg/m^3]
Thermal Conductivity (liquid)	0.15	[W/m°C]
Thermal Conductivity (solid)	0.25	[W/m°C]

Table 13: High temperature PCM material characteristics

For simplicity, the PCM storage operating between the DC and the TCS will be referred to as PCM, while the one operating between the TCS and the DHN will be called PCM_2.

In this scenario, 5% of the waste heat is recovered; consequently, the TCS volume will be 191 m³, as in Scenario 1.

Once the volume and storage capacity of the TCS are established, the required volume of PCM needed to fully charge the TCS is calculated. A total of 291.26 m³ of PCM material is required, which is divided into 12 containers of 24.27 m³ each. This configuration keeps the volume below that of a standard 20-foot container, enabling transportability. A 20-foot container has a volume of approximately 32 m³, so it would be filled to 75.85%, leaving space for auxiliary components. Once charged, the PCM containers can be transported near the TCS and charge it through the high-temperature heat pump. Each PCM container charges one TCS container, ensuring continuous charging of the thermochemical storage.

This arrangement also allows for independence among the containers, meaning that it is not necessary to have 12 different PCM containers simultaneously. When a container is fully charged, it can be returned near the data centre to begin its charging phase again. This approach can reduce the total amount of PCM material required in the system.

Regarding PCM_2, it has a total volume of 415.84 m³, which is divided into 18 containers of 23.1 m³ each. This keeps the volume below 80% of a standard 20-foot commercial container. Since the number of PCM_2 containers differs from that of the TCS containers, each TCM container charges more than one PCM_2 container.

The PCM_2 discharged temperature is higher than the supply of the DHN, so the discharge takes place directly, without the use of a heat pump. The energy consumption during this phase is therefore limited to that of any circulation pumps, which have not been considered so far.

2.2.4. Scenario 4

Scenario 4 refers to the same component arrangement as Scenario 3. However, in this case, all the heat is recovered during the months from June to September. This recovered and stored heat is then discharged into the district heating network between November and February.

In this scenario, unlike Scenario 2, where the TCS was directly connected to the DC, causing issues related to continuous charging, using the PCM, which does not have problems with non-continuous charging, eliminates this issue.

Regarding the characteristics of PCM_2, they will not be repeated here as they are the same as in Scenario 3.

Analysing the required PCM volume to recover all the waste heat from the DC, a total volume of 6,015.9 m³ is obtained. This is divided into 381 containers of 15.79 m³ each, allowing the use of standard 20-foot commercial containers filled to 49.34% capacity. The charging phase lasts 7 hours, and the total hours during which heat recovery occurs amount to 2,667. Once the charging of the PCM containers is complete, they can be transported near the TCS to transfer heat into the seasonal storage.

The TCS volume required to store all the recovered heat is 3,945.1 m³, divided into 127 containers of 31.06 m³ each. Therefore, once three PCM containers arrive near the TCS, the complete charging of one module can proceed. After the charging phase of the single TCM module is completed, the PCM containers become available again for a new heat on wheel cycle. Regarding PCM_2, its total volume is 8,589.2 m³, divided into 381 containers of 22.54 m³ each. This subdivision also allows the use of standard 20-foot commercial containers filled to 70.45% capacity.

The discharge phase of one TCM module lasts 15 hours, during which three PCM_2 modules are charged. The discharge phase of the PCM_2 containers takes place during the period from November to February. The discharge phase ends on February 20th, encompassing 2,667 hours during the chosen period (93% of the total hours between November and February). In this scenario, 130.92 kW are continuously supplied to the DHN for 2,667 hours.

2.3. Results

The numerical results of the various scenarios are presented in this section. The results related to the TCM storage; TCS system will be shown first, followed by those concerning the PCM storage in the scenarios where it is used, and finally, the overall system results will be presented. The values obtained should be considered as preliminary and are intended to highlight the potential of the simulation tool in modelling different scenarios with various interconnected components.

The Table 14 summarises the main parameters of the TCS system for the different scenarios.

Parameter	Value				Unit
	Scenario 1	Scenario 2	Scenario 3	Scenario 4	
TCS capacity	19.1	500.59	19.1	394.51	[MWh]
TCS total volume	191	5006	191	3945.1	[m^3]
TCS n° container	13	381	12	127	[-]
TCS container volume	14.69	13.14	15.92	31.06	[m^3]
TCS charge duration	8	7	15	21	[h]
TCS discharge duration	10	7	15	15	[h]

Table 14: TCS results

The Table 15 and Table 16 summarise, respectively, the main parameters of the PCM and PCM_2 storage systems for the different scenarios.

Parameter	Value		Unit
	Scenario 3	Scenario 4	
PCM capacity	16.75	345.91	[MWh]
PCM total volume	291.26	6015.9	[m^3]
PCM n° container	12	381	[-]
PCM container volume	24.27	15.79	[m^3]
PCM charge duration	11	7	[h]

PCM discharge duration	8	7	[h]

Table 15: PCM results

Parameter	Value		Unit
	Scenario 3	Scenario 4	
PCM_2 capacity	21.13	436.46	[MWh]
PCM_2 total volume	415.84	8589.2	[m^3]
PCM_2 n° container	18	381	[-]
PCM_2 container volume	23.1	22.54	[m^3]
PCM_2 charge duration	10	5	[h]
PCM_2 discharge duration	15	7	[h]

Table 16: PCM_2 results

The Table 17 presents the results related to different scenarios, comparing the energy performances.

Parameter	Value				Unit
	Scenario 1	Scenario 2	Scenario 3	Scenario 4	
PCM charge consumption	-	-	2.04	55.66	[MWh]
TCS charge consumption	9.12	233.89	5.7	117.78	[MWh]
TCS discharge consumption	5.33	153.47	-	-	[MWh]
PCM2 charging consumption	-	-	5.85	120.85	[MWh]
Total consumption	14.45	387.36	13.59	294.3	[MWh]

Energy in DHN	20.61	553.94	16.9	349.17	[MWh]
Energy-saving density	107.93	110.65	88.51	88.51	[kWh/m^3]
Efficiency	1.43	1.43	1.24	1.19	[-]
Degree of DHN demand by WH	0.03	0.68	0.02	0.43	[%]

Table 17: Results

Specifically, the metric "Energy Saving Density" was used to represent the ratio between the energy injected into the district heating network, which corresponds to the energy savings for the plant, as it does not need to produce this energy, and the volume of TCS required to provide that energy through seasonal storage. Efficiency was calculated as the ratio between the energy delivered to the DHN and the total work required to achieve it.

Finally, the percentage of the DHN demand covered by the waste heat recovered from the DC was reported. The mismatch in scale between the DC and the DHN results in a coverage rate of less than 1%. This value is expected to increase when analysing waste heat sources and end-users of comparable sizes.
In this case, the analysis was conducted with these parameters because evaluating a DC in the megawatt range would have resulted in storage volumes that are too large to manage at this stage of the project.

3. Conclusion

This deliverable has provided a comprehensive overview of the conceptual design developed within the THUNDER project, with a particular focus on the integration of seasonal TES systems and innovative strategies for the recovery and transport of waste heat from DC. The analysis demonstrated that adopting a mobile storage system based on PCM offers an effective, safe, and flexible solution to overcome the limitations imposed by the physical distance between heat sources and thermal users.

The “Heat on Wheels” approach, which involves the use of mobile modules for heat transport, allows system design to be decoupled from the need for direct hydraulic connections. This opens new possibilities for integrating waste heat sources with urban district heating networks or other local thermal users. In particular, the use of PCM has proven advantageous for managing operating temperatures and fluid pressures, while ensuring ease of transport and compliance with safety and space constraints typical of urban and residential environments.

The comparison of different replicability scenarios highlighted the scalability and adaptability of the THUNDER solution to various contexts, both in terms of spatial configuration and energy management strategies. The integration with a seasonal storage system based on TCM, although more complex from a technical standpoint, enables maximisation of energy efficiency and storage density, making it particularly suitable for industrial settings or concentrated thermal demands.

A central element of this work was the development of an advanced numerical tool in Python, capable of modelling the entire THUNDER energy chain. This tool enabled dynamic simulation of each component and its interactions, providing essential support for the design of the Varna demonstrator and for evaluating replicability in other contexts. Its modularity and customisable input parameters make it a powerful resource for future scenario analysis and control strategy optimisation.

In summary, the work carried out in Task 1.1.2 has laid a solid foundation for the demonstrator’s implementation and the broader dissemination of the THUNDER concept, contributing significantly to the transition toward a more efficient, sustainable, and resilient energy system.

References

[1] One Building. Varna Weather Data. https://climate.onebuilding.org/sources/default.html n.d.

[2] Ebrahimi K, Jones GF, Fleischer AS. A review of data center cooling technology, operating conditions and the corresponding low-grade waste heat recovery opportunities. Renew Sustain Energy Rev 2014;31:622–38. https://doi.org/10.1016/j.rser.2013.12.007.

[3] Mohapatra D, Nandanavanam J. Salt in matrix for thermochemical energy storage - A review. Mater Today Proc 2023;72:27–33. https://doi.org/10.1016/j.matpr.2022.05.453.

[4] Chen Z, Zhang Y, Zhang Y, Su Y, Riffat S. A study on vermiculite-based salt mixture composite materials for low-grade thermochemical adsorption heat storage. Energy 2023;278:127986. https://doi.org/10.1016/j.energy.2023.127986.

[5] Zbair M, Bennici S. Survey Summary on Salts Hydrates and Composites Used in Thermochemical Sorption Heat Storage: A Review. Energies 2021;14:3105. https://doi.org/10.3390/en14113105.

[6] Rehman AU, Shah MZ, Rasheed S, Afzal W, Arsalan M, Rahman HU, et al. Inorganic salt hydrates and zeolites composites studies for thermochemical heat storage. Z Für Phys Chem 2021;235:1481–97. https://doi.org/10.1515/zpch-2021-3012.

[7] Mahon D, Claudio G, Eames PC. An experimental investigation to assess the potential of using MgSO 4 impregnation and Mg 2+ ion exchange to enhance the performance of 13X molecular sieves for interseasonal domestic thermochemical energy storage. Energy Convers Manag 2017;150:870–7. https://doi.org/10.1016/j.enconman.2017.03.080.

[8] Gao N, Deng L, Li J, Huang H, Zhou B, Zhou Y. Multi-form heat storage performance of expanded graphite based CaCl2 composites for low-grade heat source. Energy Rep 2022;8:12117–25. https://doi.org/10.1016/j.egyr.2022.09.051.

[9] Miao Q, Zhang Y, Jia X, Li Z, Tan L, Ding Y. MgSO4-expanded graphite composites for mass and heat transfer enhancement of thermochemical energy storage. Sol Energy 2021;220:432–9. https://doi.org/10.1016/j.solener.2021.03.008.

[10] Airò Farulla G, Cellura M, Guarino F, Ferraro M. A Review of Thermochemical Energy Storage Systems for Power Grid Support. Appl Sci 2020;10:3142. https://doi.org/10.3390/app10093142.

[11] Yang T, Liu W, Kramer GJ, Sun Q. Seasonal thermal energy storage: A techno-economic literature review. Renew Sustain Energy Rev 2021;139:110732. https://doi.org/10.1016/j.rser.2021.110732.

[12] Xu J, Wang RZ, Li Y. A review of available technologies for seasonal thermal energy storage. Sol Energy 2014;103:610–38. https://doi.org/10.1016/j.solener.2013.06.006.